Title

THE CLASSICAL-LIMIT S-MATRIX and ORBITAL DYNAMICS IN SEMECLASSICAL COULOMB EXCITATION THEORY

Author

Guidry, M.W.

Publication Date

1977-07-13

Submitted to Nuclear Physics A

LBL-4363
Preprint

THE CLASSICAL-LIMIT S-MATRIX AND ORBITAL DYNAMICS IN SEMICLASSICAL COULOMB EXCITATION THEORY

M. W. Guidry, R. Donangelo, J. O. Rasmussen, and J.-P. Boisson

July 13, 1977

Prepared for the U. S. Energy Research and Development Administration under Contract W-7405-ENG-48

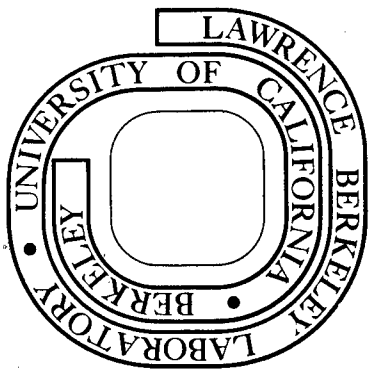

DISCLAIMER

THE CLASSICAL-LIMIT S-MATRIX AND ORBITAL DYNAMICS IN SEMICLASSICAL COULOMB EXCITATION THEORY*

M. W. Guidry
Lawrence Berkeley Laboratory, Berkeley, California 94720
and
Department of Physics and Astronomy
University of Tennessee, Knoxville, Tennessee 37916†

and

R. Donangelo and J. O. Rasmussen
Lawrence Berkeley Laboratory, Berkeley, California 94720

and

J.-P. Boisson
Institute des Sciences Nucleaires de Grenoble,
BP 257 Centre de Tri - 38044 Grenoble Cedex, France†
and
Lawrence Berkeley Laboratory, Berkeley, California 94720

ABSTRACT

A previously introduced formalism employing the classical limit of the quantum-mechanical S-matrix for Coulomb excitation is extended by applying direct numerical evaluation of the S-matrix in an integral representation, and by employing complex classical trajectories in a saddle-point approximation to the integral S-matrix. The equations of motion are parametrized in terms of dimensionless quantities, and the dynamics of the system in the classical limit are discussed. A detailed consideration of the classical equations of motion and comparisons

---

*Work performed under the U.S. Energy Research and Development Administration

†Present address.

to exact quantum-mechanical calculations and to conventional semi-classical calculations for backward scattering are carried out. The results suggest that the classical-limit S-matrix method is able to almost exactly reproduce both the amplitude and the phase of the quantum-mechanical S-matrix, even for projectiles as light as protons, and that this approach should be a better approximation for heavy-ion multiple Coulomb excitation than earlier semiclassical methods, due to a more accurate description of the classical orbits in the combined monopole-quadrupole field of the target nucleus. The indicated corrections due to the approximate orbital dynamics in the Alder-Winther-de Boer calculations increase with spin, but are generally < 20% for states easily measured, which is in agreement with recent experimental results setting an upper limit on the magnitude of these corrections.

1. Introduction

The recent availability of very heavy ions has made it possible to populate high spin states ($I \simeq 20\ \hbar$) with multiple Coulomb excitation processes. Exact partial-wave, coupled-channel calculations are possible for Coulomb excitation with light projectiles,[1] but such calculations are not feasible at present for heavy-ion systems. The most common approach to this problem has used the semiclassical methods developed by Alder and Winther[2] (A-W) and embodied in the widely-used Winther-deBoer code[3] to calculate multiple Coulomb excitation probabilities. In this approach the internal degrees of freedom are treated quantum-mechanically but the projectile dynamics are taken as that of a classical particle on an energy-symmetrized hyperbola.

As Alder et al. have shown,[4-6] this accounts quite nicely for first-order processes, but higher-order processes such as multiple E2 or E4 excitation may necessitate corrections to semiclassical calculations. Historically, these corrections have been termed "quantal" or "quantum-mechanical" corrections by experimentalists and theorists alike, since they represented differences between exact (i.e. quantal) calculations and the approximate semiclassical ones. Alder has pointed out, however, that a significant part of this "quantal" correction is independent of $\hbar$ and therefore is not a true quantum-mechanical effect at all, but rather is due to the neglect of the electric quadrupole potential in calculating the semiclassical trajectory.[6] The weight of the evidence presented in this paper supports this point of view, and we shall refer to these effects as orbital dynamics effects. Any effects that are of a specifically quantum dynamical origin (in a sense to be specified later) are probably beyond the range of this method, but the results

presented here suggest that for heavy-ion systems those effects must be quite small.

Initial attempts to account for the "quantal" corrections arising from the use of approximate orbital dynamics have involved extrapolations from exact light-ion calculations[4-7] and sophisticated energy and angular-momentum symmetrizations in the semiclassical limit.[8] In refs. 9 and 10) a third approach was introduced, using classical limit S-matrix (CLSM) methods originally developed in atomic and molecular scattering problems.[11] It was suggested[10] that this approach might be capable of supplying corrections due to the semiclassical orbital dynamics. In this paper we apply recently introduced refinements to the CLSM method,[12-14] and provide evidence that this approach can be used with confidence to determine excitation probabilities for heavy-ion multiple Coulomb excitation.

2. Coulomb Excitation of a Deformed Rotor

The classical limit S-matrix for Coulomb excitation of a deformed rotor has been formulated previously for the case of purely real classical trajectories.[9,10] The approach adopted in this paper is a more comprehensive one which can be reduced to that of ref. 10) by approximation.[13,14] The spirit is the same as that of ref. 10) however, and the reader is directed there for much of the nomenclature and many of the basic ideas employed here. We also note that in ref. 12) a more general problem is considered which includes the effect of a complex nuclear potential as well as the electromagnetic interaction on rotational excitation. The reader is also referred to other recent applications in nuclear physics of methods similar to those described here[15-18] and to a recent book devoted to related topics.[19]

a. Hamiltonian and Equations of Motion

We consider a spherical projectile incident on an even-even deformed nucleus in its ground state, neglecting any projectile excitation. The Hamiltonian of the projectile-target system in the center of mass coordinate system may be written[20]

$$H(p_r,j,M,r,q_j,q_M) = \frac{p_r^2}{2m} + \frac{j^2}{2\mathcal{I}} + \frac{J^2+j^2-2M^2+2(J^2-M^2)^{1/2}(j^2-M^2)^{1/2}\cos q_M}{2mr^2}$$

$$+ V(r,\chi) \qquad (1)$$

where r is the distance between centers of projectile and target, p_r the relative radial momentum, j the rotational angular momentum of the target, J the total angular momentum of the system, M the helicity (i.e., the projection of the angular momentum of the target onto the relative velocity direction), m the reduced mass of the system, $\mathcal{I}$ the moment of inertia of the target, $V(r,\chi)$ the interaction potential between the two nuclei, and χ is the angle between the rotor axis and the line connecting its center to the center of the projectile. The variables conjugate to j and M are the angles q_j and q_M respectively, and χ is given in terms of these canonical variables by[20]

$$\cos\chi = (1 - M^2/j^2)^{1/2} \cos q_j \ .$$

For the purposes of this paper it will not be necessary to consider the full Hamiltonian of eq. (1). Instead we study a simpler case which will be more amenable to physical interpretation and require less numerical effort. First, since we are considering only Coulomb excitation here, we drop the complex nuclear potential used in ref. 12). In addition,

for simplicity we drop any E4 contribution to the excitation (these restrictions can be easily removed[10,12]). Then the interaction potential takes the form

$$V(r,\chi) = \frac{Z_p Z_t e^2}{r} + \frac{Z_p Q_0^2 e^2}{2r^3} P_2(\cos\chi)$$

where Z_p and Z_t are the atomic numbers of the projectile and target respectively, e is the electronic charge, $Q_0^{(2)}$ is the intrinsic electric quadrupole moment of the target nucleus, and $P_2(\cos\chi)$ is the second-order Legendre polynomial.

As in previous cases[10,12,13] we will further confine ourselves to a simple model in which we calculate the S-matrix for the $\ell = 0$ incident partial wave only. From eq. (1), this implies that M must be identically zero, and the Hamiltonian reduces to the simple form

$$H(p_r,p_\chi,r,\chi) = \frac{p_r^2}{2m} + \left(\frac{1}{2\mathcal{I}} + \frac{1}{2mr^2}\right)p_\chi^2 + \frac{Z_p Z_t e^2}{r} + \frac{Z_p e^2 Q_0^{(2)}}{2r^3} P_2(\cos\chi) \qquad (1')$$

since now $q_j = \chi$, and where we define $p_\chi = j$. The variables appearing in the Hamiltonian are illustrated in Fig. 1.

From (1') the classical equations of motion are

$$\dot{r} = P_r/m \tag{2-a}$$

$$\dot{P}_r = \frac{P_\chi^2}{mr^3} + \frac{Z_p Z_t e^2}{r^2} + \frac{3Z_p e^2 Q_0^{(2)}}{2r^4} P_2(\cos \chi) \tag{2-b}$$

$$\dot{\chi} = \left(\frac{1}{\mathcal{I}} + \frac{1}{mr^2}\right) P_\chi \tag{2-c}$$

$$\dot{P}_\chi = -\frac{3Z_p e^2 Q_0^{(2)}}{2r^3} \sin \chi \cos \chi \tag{2-d}$$

The initial conditions for the integrations are

$$r_i = \text{large} \tag{3-a}$$

$$P_{r_i} = -\sqrt{2m\left(E_{cm} - \frac{Z_p Z_t e^2}{r_i}\right)} \tag{3-b}$$

$$\chi_i = \chi_0 \quad \text{in the interval } [0,\pi] \tag{3-c}$$

$$P_{\chi_i} = 0 \tag{3-d}$$

where E_{cm} is the translational energy in the center of mass system. The classical action Φ is defined as the time integral of the Lagrangian and may be determined from the equation

$$\dot{\Phi} = -1/\hbar \ (r\dot{P}_r + \chi\dot{P}_\chi). \tag{4}$$

b. The Classical-Limit S-Matrix

As shown in refs. 13,14), the classical limit (classical action >> $\hbar$) of the quantum mechanical S-matrix for rotational scattering to a spin I in this model may be written in the form

$$S_{0\to I}^{J=0} = \frac{\sqrt{2I+1}}{2} \int_0^{\pi} P_I(\cos \bar{\chi}) \sqrt{\sin \chi_0 \sin \bar{\chi} \frac{d\bar{\chi}}{d\chi_0}} \; e^{i\phi'} \, d\chi_0 \qquad (5)$$

The phase ϕ' is given in units of $\hbar$ by

$$\begin{aligned} \phi' = & -\frac{1}{\hbar} \int [r(t)dp_r(t) + \chi(t)dp_\chi(t)] + \frac{1}{\hbar} \bar{\chi} p_\chi \\ & + \frac{1}{\hbar} \int_{\tilde{r}_T}^{r} \tilde{p}_r d\tilde{r} + \sigma_0(\eta_0) + \sigma_I(\eta_I). \end{aligned} \qquad (6)$$

We note here that the classical-limit S-matrix nomenclature arises from the fact that we are evaluating amplitudes (not probabilities), so quantum superposition is implicit in the integral (5), but all quantities in (5), and (6) are evaluated by classical methods. In the last equation $\sigma_0(\eta_0)$ and $\sigma_I(\eta_I)$ are the Coulomb phase shifts in the entrance and exit channels respectively, with η defined in eq. (16-a), $\tilde{p}_r$ is the radial momentum along an elastic trajectory governed by the Coulomb potential $Z_p Z_T e^2/r$ such that the energy E along this trajectory equals the total energy of the system, i.e.

$\tilde{p}_r$ is defined by

$$E = \frac{\tilde{p}_r^{\,2}}{2m} + \frac{1}{2}\left(\frac{1}{\mathcal{I}} + \frac{1}{m\tilde{r}^2}\right)p_\chi^2 + \frac{Z_p Z_T e^2}{\tilde{r}}$$

where p_χ takes its asymptotic value, $\tilde{r}$ is the position along the elastic trajectory at which $\tilde{p}_r$ is evaluated in eq. (6), and $\tilde{r}_T$ is the turning point of the radial motion for the elastic collision, that is $\tilde{p}_r(\tilde{r}_T, p_\chi, E) = 0$. Finally the quantity $\bar{\chi}$ is defined by the transformation[21]

$$\bar{\chi} = \chi + \int_{r_T}^{r} \frac{\partial \tilde{p}_r}{\partial p_\chi}\, d\tilde{r} = \chi - mp_\chi \int_{\tilde{r}_T}^{r} \left(\frac{1}{\mathcal{I}} + \frac{1}{m\tilde{r}^2}\right) \frac{d\tilde{r}}{\tilde{p}_r} \quad . \tag{7}$$

The variable $\bar{\chi}$ can be seen, by differentiation of Eq. (7), to be constant in the final asymptotic region; in that region it can be written[13] as $\chi = \chi - \omega t$, where $\omega = p_\chi/\mathcal{I}$ is the angular velocity of the target.

Transformation (7) is necessary to remove an oscillatory time dependence of the variable χ in the asymptotic region. It is closely related to the unitary transformation from the Schrödinger representation into the interaction representation in quantum mechanics, which is also introduced to transform away an oscillatory time dependence. The transformation prescription described here was shown numerically to yield an S-matrix element which was independent of the initial and final values of the radial coordinate in the asymptotic regions.

The quantities appearing in eq. (5) may be determined by numerical integration of the classical equations of motion (eq. 2,4) with the appropriate initial conditions (eq. 3). We will then evaluate the integral representation (5) in two different ways: 1) direct numerical integration,[13,14] and 2) saddle-point or stationary-phase approximations.[9-12]

As shown in refs. 13, 14), eq. (5) may be accurately integrated for nuclear systems using standard numerical methods. When this approach is used in this paper we will refer to it as the integral method. It is a classical-limit approach because eq. (5) is obtained as a generalized WKB solution to the Schrödinger equation for the system.

The integral in eq. (5) may also be evaluated by stationary phase or saddle-point methods,[11] yielding results analogous to those of ref. 10). When this approach is used in this paper we will term it the saddle-point method. To show the connection between the integral and saddle-point methods we first approximate the Legendre polynomial appearing in (5) by the asymptotic form

$$P_I(\cos\bar{\chi}) \approx 2\cos\left[(I+1/2)\bar{\chi} - \pi/4\right] \Big/ \sqrt{(2I+1)\sin\bar{\chi}}$$

$$= \frac{e^{i[I+1/2)\bar{\chi} - \pi/4]} + e^{-i[(I+1/2)\bar{\chi} - \pi/4]}}{\sqrt{(2I+1)\sin\bar{\chi}}} \quad . \tag{8}$$

Now, using the fact that χ_0 and $\pi-\chi_0$ result in opposite final angular momenta, and that the spin I must be even for a rotor with axial symmetry we find[13]

$$S_{0\to I}^{J=0} \approx \frac{1}{\sqrt{\pi}} \int_0^{\pi} \sqrt{\sin\chi_0 \frac{d\bar{\chi}}{d\chi_0}} \quad e^{i[\phi' - (I+1/2)\bar{\chi}]}\, d\chi_0 \ . \tag{9}$$

In the classical limit the integrand of eq. (9) will be highly oscillatory and the integral will receive contributions only from those points where the phase is stationary (saddle points). For the present zero impact parameter case, only one or two saddle points will make significant contributions to the integral.

Expanding to second order at the saddles and using the methods of refs. 10,12) we obtain the so-called primitive classical S-matrix for classically allowed transitions (real saddle points)[11)]

$$S_{0\to I}^{Prim} \cong i\left\{\sqrt{|\bar{p}_1|}\, e^{i(\Phi_1 + \pi/4)} + \sqrt{|\bar{p}_2|}\, e^{i(\Phi_2 - \pi/4)}\right\} . \qquad (10)$$

Where the two terms of eq. (10) arise from the stationary phase condition and

$$\sqrt{\bar{p}_k} = \sqrt{\frac{2 \sin\bar{\chi}_k}{\frac{1}{\hbar}\left(\frac{\partial I(\chi_0)}{\partial \chi_0}\right)_{\bar{\chi}_k}}} \qquad k = 1,2 .$$

with $\bar{\chi}_k$ the initial orientation angles leading to a given final spin, and Φ_k the classical action for an initial orientation $\bar{\chi}_k$. As discussed below, for classically forbidden transitions (complex saddle points), only one term of (10) will contribute to the excitation probability.

Equation (10) is valid for well-separated points of stationary phase. For coalescing saddle points the 2nd-order expansion is no longer adequate. A uniform expression valid in all regions is obtained by mapping the phase onto a suitably chosen cubic polynomial, which results in a uniform approximation for the S-matrix.[12,22,23)]

$$S_{0\to I}^{USCA} = -\sqrt{\pi}\, e^{i(\Phi_1 + \Phi_2)/2} \left[(\sqrt{\bar{p}_1} + \sqrt{-\bar{p}_2})\,\xi^{1/4}\, Ai(-\xi) - i(\sqrt{\bar{p}_1} - \sqrt{-\bar{p}_2})\, 1/\xi^{1/4}\, Ai'(-\xi)\right] \qquad (11)$$

where

$$\xi = [3/4\ (\Phi_2 - \Phi_1)]^{2/3}. \qquad (12)$$

The $Ai(-\xi)$ and $Ai'(-\xi)$ represent respectively the complex Airy function and its first derivative. Equation (11) is valid both for forbidden and allowed transitions. For classically forbidden transitions in the saddle-point approximation all of the variables in (10) and (11) may be complex. The saddle-point method with the Airy uniform approximation will be denoted the Uniform Semiclassical Approximation (USCA).[10,12,23]

In ref. 10), real trajectories were used to construct the quantum number function (defined as the final spin I as a function of initial orientation χ_0) and the phase. The classically forbidden processes were then approximated by a quadratic expansion of these functions into the complex plane. This approximation is removed here (and in ref. 12), since we are evaluating the full complex trajectory for the forbidden transitions. The real quantum number function $\hat{I}(\chi_0)$ discussed in ref. 10) now generalizes to a complex function, and the asymptotic quantization conditions are

$$\begin{aligned} &\mathrm{Re}[\hat{I}(\chi_0)] = I + 1/2 \qquad (I = \text{even integer}) \\ &\mathrm{Im}[\hat{I}(\chi_0)] = 0. \end{aligned} \tag{13}$$

where $\hat{I}(\chi_0) \equiv p_{\chi}^{\text{final}}(\chi_0)$.

For this zero impact parameter approximation the excitation probability in the channel of interest is given by the square modulus of the appropriate S-matrix element

$$P_{0\to I} = |S_{0\to I}^{J=0}|^2. \tag{14}$$

For all numerical calculations of probabilities with the saddle-point approximation we have used the uniform expression (11) inserted into eq. (14). However, it will be of conceptual utility to write explicitly the formula for the primitive semiclassical probability. From (10) and (14) we have [10-12]

$$P_{prim} \simeq P_1 + P_2 + 2\sqrt{P_1 P_2}\,\sin(\Delta\Phi)$$

(classically allowed states) (15-a)

$$P_{prim} \simeq P e^{-2\,\mathrm{Im}\Phi}$$

(classically forbidden states). (15-b)

where $\Delta\Phi = \Phi_2 - \Phi_1$

The interference structure for the classically allowed states in (15-a) arises from the coherent contribution of two real saddle points (initial orientation angles) to the probability for a given state. For classically forbidden states in Coulomb excitation the phases Φ_1 and Φ_2 in eq. (10) are complex conjugates and purely imaginary. This implies that one of the contributions to the probability would be exponentially increasing, and by physical arguments should not contribute to the forbidden probability, leaving only a single exponentially damped term in (15-b). More rigorously one can show that the topology of saddles changes in going from allowed to forbidden transitions, and that the steepest descent integration path only traverses the physically-acceptable saddle point.[23] The different paths are shown in Fig. 2.

c. Relation Between Integral and Saddle-Point Methods

Since we are using in this paper two distinct but related techniques (the integral method and the saddle-point method) it is useful at this point to briefly summarize the similarities and differences between these two approaches. Both methods are classical-limit methods in that they introduce into the quantum-mechanical S-matrix a phase (the classical action) which is the time integral of the classical Lagrangian. The validity of this approximation is predicated on the classical action being much larger than $\hbar$, the characteristic quantum-mechanical unit of action; and the classical limit may be formally defined as the limit $\hbar \to 0$. The differences in the two approaches lie in the methods used to evaluate the resulting integral representation of the classical-limit S-matrix: direct numerical integration, or analytical solutions utilizing asymptotic expansions and saddle point techniques.

The saddle point method is elegant and conceptually enlightening. It is the mathematically correct way to speak of classical trajectories since in this formalism the saddle points define the stationary-action paths for the system, which are precisely the classical paths in Hamiltonian dynamics. In the present simple model the saddle points are not difficult to find, but in complicated applications involving more degrees of freedom (for instance the extension to the non-zero impact-parameter case) the search for the points of stationary phase (saddle points) could become a formidable technical problem. In addition, the uniform prescription (USCA) of eq. (11) is neither unique, nor globally valid, although it should be quite good for heavy-ion Coulomb excitation of high-spin states

in the present model. For example, it isn't valid for more than two coelescing points of stationary phase, nor is it particularly good for situations where angular momentum transfer to even the lowest excited state is classically forbidden — a case in which a uniform Bessel approximation is known to be superior to the Airy approximation.[18)]

The integral method avoids these difficulties since it evaluates eq. (5) directly by numerical means rather than by seeking approximate analytical solutions. The price that must be paid involves renouncing some of the conceptual enlightenment inherent in the saddle point method. In the integral approach the trajectories are more properly thought of as mathematical devices to calculate the phases and amplitudes in eq. (5)--it is only through the stationary phase evaluation of eq. (5) that one actually selects the classical paths, those for which the classical action is an extremum. Furthermore, while all representations are equivalent for the saddle-point method, it is imperative for the integral approach that a proper representation be chosen for the classical-limit wavefunction.[13,14)] Otherwise spurious singularities may be introduced into the wavefunction. Eq. (7) is an example of a transformation which meets this requirement for a wide variety of cases.[14)]

It should also be noted that for a case such as the one being considered here where the potential is real and slowly varying, all trajectories used in calculating the amplitudes and phases in eq. (5) are real, though the trajectories in the saddle-point method may become complex. This may be understood from Fig. 2. For real potentials, a complex trajectory is associated with a classically forbidden process in which the point(s) of stationary phase move into the complex plane (Fig. 2-b). In the saddle-point or steepest-descent integration method one deforms the path of integration (the dotted line of Fig. 2-b) to pass over the saddle point(s). Since the point of stationary phase is complex, the trajectory is complex. In the integral method the integration path,

indicated by the solid line in Fig. 2-b, is along the real axis, irrespective of the position of the saddle points. By the Cauchy integral theorem we are free to take any integration path we wish, provided that the function is analytic, and that we don't pass around any poles. Therefore either path in Fig. 2-b may be used to evaluate the integral if there are no poles in the region bounded by the dotted and solid integration paths. As discussed in ref. 12), the trajectories in both the saddle-point and integral methods are complex if the potential is complex, and the clear distinction between allowed and forbidden processes is erased.

In principle the integral and saddle-point methods should be of comparable (but not necessarily identical) accuracy since they are both correct to the same order of $\hbar$, provided that a proper uniform expression is used in the saddle point approximation, and that the integral method uses an appropriate representation. For small angular momentum transfer the integral method is more accurate than the USCA for the cases studied here.[13,14] It is not clear how much of this difference is due to the Airy uniform approximation in the USCA and how much is more fundamental. Presumably an improvement in the USCA accuracy could be obtained by using a Bessel rather than Airy function mapping in the uniform expression (11).[18] Because the integral expression works so well in these cases, however, we have not investigated this possibility. For heavier systems (e.g., $^{40}Ar + ^{238}U$) the integral and USCA results are very similar in the present simple model. In Fig. 3 we indicate schematically the relationships among the various methods discussed in this paper.

3. Semiclassical and Classical-Limit Dynamics

a. Parametrized Equations of Motion

It is convenient to define the following standard dimensionless quantities for Rutherford trajectories

$$\eta = \frac{Z_t Z_p e^2}{\hbar v_i} \qquad \text{(Sommerfeld parameter--monopole-monopole interaction strength)} \qquad (16\text{-a})$$

$$a = \frac{Z_t Z_p e^2}{m v_i^2} \qquad \text{(1/2 distance of closest approach for a head-on trajectory)} \qquad (16\text{-b})$$

$$\xi_{02} = \eta \frac{\Delta E_2}{2E_{cm}} \qquad \text{(adiabaticity parameter)} \qquad (16\text{-c})$$

$$\bar{q}_2 = \frac{Z_p e^2 Q_0^{(2)}}{4\hbar v_i a^2} \qquad \text{(multipole-monopole interaction strength)} \qquad (16\text{-d})$$

where v_i is the initial relative velocity, ΔE_2 is the energy of the rotor 2^+ state, and $Q_0^{(2)}$ is the intrinsic quadrupole moment of the target nucleus.

In addition, following Massmann we define two other dimensionless quantities by the relations[23]

$$\zeta \equiv \xi_{02}\bar{q}_2 = (3/4)\left(\frac{Q_0^{(2)}}{Z_t}\right)\Big/\left(\frac{Q}{m}\right) \qquad (17\text{-a})$$

$$\Lambda \equiv \bar{q}_2/\eta = \left(\frac{Q_0^{(2)}}{4Z_t a^2}\right) \qquad (17\text{-b})$$

The significance of the variables ζ and Λ will be discussed subsequently. In the equations of motion we introduce the following dimensionless variables

$$\tau = v_i t/a \qquad (18\text{-a})$$

$$S = r/a \qquad (18\text{-b})$$

$$\tilde{I} = \frac{P_\chi}{\hbar} \frac{1}{2\bar{q}_2} \tag{18-c}$$

$$P_S = \frac{P_r}{mv_i} \quad . \tag{18-d}$$

The dimensionless variable τ measures the time in units of the time necessary to cover one-half the distance of closest approach at initial asymptotic velocity. The variable S measures the radial distance in units of half the distance of closest approach for a Rutherford trajectory with zero impact parameter. Since $2\bar{q}_2$ is the maximum classical angular momentum that may be imparted in the sudden-impact limit,[10,24] $\tilde{I}$ measures the ratio of the angular momentum actually transferred to the maximum transferred in the sudden-impact limit. The dimensionless radial momentum P_S is given in units of the radial momentum before interaction.

Using the dimensionless quantities defined in eqs. (16-18), the equations of motion for the dynamical variables and the classical phase may be written as

$$\frac{dS}{d\tau} = P_S \tag{19-a}$$

$$\frac{dP_S}{d\tau} = \frac{1}{S^2} + \frac{6\Lambda}{S^4} P_2(\cos\chi) + \frac{4\Lambda^2}{S^3} \tilde{I}^2 \tag{19-b}$$

$$\frac{d\chi}{d\tau} = \left(\frac{2}{3}\zeta + \frac{2\Lambda}{S^2}\right)\tilde{I} \tag{19-c}$$

$$\frac{d\tilde{I}}{d\tau} = 3/2 \frac{\sin(2\chi)}{S^3} \tag{19-d}$$

$$\frac{d\Phi}{d\tau} = -\eta S \frac{dP_S}{d\tau} - 2\bar{q}_2\chi \frac{d\tilde{I}}{d\tau} \; . \tag{19-e}$$

b. The Nature of Semiclassical and Classical-Limit Approximations

It is important at this point to consider carefully the nature of the approximations implicit in the Alder-Winther (A-W) semiclassical method[2] and in the classical limit S-matrix method (CLSM). In the A-W approach the wavefunction is expanded on the unperturbed nuclear eigenstates, but the time dependence of the interaction potential in the resulting coupled Schrödinger equations is approximated as due to a projectile moving on a classical Rutherford trajectory. In this sense the method may be characterized as one which treats the target internal excitation degrees of freedom quantum mechanically, but which treats the projectile degrees of freedom using approximate classical dynamics. The dynamics are approximate because 1) all coupling of the projectile motion to the non-central part of the potential (e.g., the quadrupole field) is ignored, and 2) because the energy difference in the entrance and exit channels for an inelastic process is only approximately accounted for by the introduction of energy-symmetrized hyperbolas.

The validity of this approximation rests on whether the wave-packet representing a projectile in a given situation behaves as a localized particle subject to classical equations of motion and, if so, whether the deviations from a Rutherford trajectory arising from coupling to the quadrupole field and from finite energy transfer are sufficient to invalidate the approximate classical dynamics employed. The first question relates to whether there are explicit quantum dynamical effects operating which cast doubt on the concept of a classical trajectory. It is a question about phenomena which vanish in the limit $\hbar \to 0$ and which can only be fully answered in the

context of a rigorous quantum mechanical analysis. The second question concerns effects which are due to approximations in the classical dynamics employed and which are independent of $\hbar$. This question might reasonably be answered within a classical or classical-limit framework.

It is well known that the classical and quantum mechanical results coincide for Rutherford (1/r) scattering, but not for $1/r^n$ ($n > 1$) potentials. From this point of view the introduction of, e.g., a quadrupole potential has two general consequences for semiclassical theories: 1) the potential now has a short-ranged component for which classical and quantal solutions are not identical, i.e. explicit quantum-dynamical ($\hbar$-dependent) effects have been introduced, and 2) the classical ($\hbar$-independent) dynamics are affected because the scattering center is no longer a simple monopole.

In the classical limit S-matrix method one forsakes the semiclassical prescription of a quantum mechanical treatment for the internal degrees of freedom and approximate classical treatment of the projectile motion. Instead, both the internal and projectile degrees of freedom are approximated by exact classical dynamics. Although the dynamics are those of classical mechanics, one retains certain quantum-mechanical features since the superposition principle and quantized boundary conditions are implicit in the CLSM method.[11] The validity of this approximation depends upon the validity of using classical mechanics to describe both the particle and the rotor dynamics. Two things should be carefully noted: 1) If the concept of a classical trajectory is valid, the CLSM trajectories are dynamically exact, while the A-W trajectories

employ dynamical approximations. 2) The A-W treatment of the target internal degrees of freedom is a quantum-mechanical one, while the CLSM method employs an approximation which, at first glance, might seem severe.

c. The Parameters η, $\bar{q}_2$, and Λ

As Alder et al. have pointed out,[2-7] the Sommerfeld parameter η plays a critical role in assessing the validity of any semiclassical method. This is to be expected since we deduce from equations (16) that, in addition to describing the monopole-monopole interaction strength, η is the ratio of the projectile deBroglie wavelength to half the distance of closest approach for a Rutherford trajectory. Therefore η measures the spatial confinement of the projectile wave packet relative to a characteristic interaction distance, and indicates the degree to which the wave packet remains intact during the interaction with the scattering center.

Therefore, in the classical equations of motion we expect quantities involving η to play a dominant role. We first note that the possibility of calculating probabilities in any classical trajectory model depends upon the plausibility of assigning definite scattering angles to given ℓ-components of the partial-wave reaction amplitude. The mathematical steps for accomplishing this generally involve 1) replacement of the partial wave summation over discreet ℓ with an integral over continuous ℓ, 2) replacement of Legendre polynomials by asymptotic forms for larger ℓ, and 3) evaluation of the

resultant integrals by stationary-phase integration. The asymptotic forms of the Legendre polynomials are valid for large values of the total orbital angular momentum $L \approx \eta\sqrt{\varepsilon^2-1}$, where ε is the eccentricity of the hyperbolic orbit. Therefore, these forms are more accurate for large η. Similarly, since the error introduced in going from a summation to an integral in the partial wave series is proportional to the step width $1/L$, we deduce that the error in the scattering amplitude due to this approximation is of order $1/\eta$.

In the classical equations of motion (19) the most critical parameter describing the validity of the Alder-Winther semiclassical method is the $\hbar$-independent parameter Λ, the ratio of the quadrupole coupling parameter $\bar{q}_2$ to the Sommerfeld parameter η. From (19-b) we deduce that the equation of motion for the radial momentum involves only the monopole potential for $\Lambda \to 0$. Therefore Λ, which indicates the relative strength of the monopole-quadrupole interaction relative to the monopole-monopole interaction, will be a measure of the deviation of the projectile orbit from that of a pure Rutherford hyperbola. If $\Lambda << 1$, the monopole-monopole interaction determines the projectile trajectory except for a small perturbation from the monopole-quadrupole coupling. If $\Lambda \approx 1$ both the monopole and quadrupole potentials play significant roles in the trajectory dynamics. If $\Lambda >> 1$, the projectile trajectory in the interaction region would be a function primarily of the quadrupole field.

The rather accurate results of A-W semiclassical calculations[2] in most applications are a consequence of the dominant role played by the monopole field for Coulomb excitation in real nuclei. For all but the very lightest projectiles, $\Lambda \lesssim 0.1$ for sub-barrier interactions, and an energy-symmetrized hyperbola computed from the monopole-monopole interaction is a good approximation to the actual trajectory.

For the CLSM method the most critical parameters determining the validity of the approximation are η and $\bar{q}_2$ separately rather than the ratio $\Lambda = \bar{q}_2/\eta$. While Λ is independent of $\hbar$, η and $\bar{q}_2$ are each inversely proportional to $\hbar$. If η is large the approximation of a classical trajectory for the projectile dynamics becomes more accurate. Similarly, the validity of the classical rotor description of the internal eigenstates should increase as the rotational quantum numbers get larger, and hence be favored by large angular momentum transfer in heavy-ion reactions. Since $2\bar{q}_2$ is the maximum classical angular momentum that can be transferred in the sudden limit, $\bar{q}_2$ is an approximate measure of the validity of the classical rotor approximation.

We may view this in another way by noting that the general condition for the validity of a classical description for a degree of freedom is that[19)]

$$\Phi/\hbar >> 1$$

where Φ is the classical action associated with the degree of freedom. From 19-e it is easily shown that the classical action in units of $\hbar$ associated with the rotational degree of freedom is approximately proportional to $2\bar{q}_2$ and will be large for large values of $\bar{q}_2$.

Therefore, both the CLSM and the A-W semiclassical methods are favored by large values of η, but differ in their dependence on $\bar{q}_2$. The CLSM should be favored by large values of $\bar{q}_2$ (large angular momentum transfer) which make the classical rotor approximation more reasonable. Conversely, the A-W semiclassical method should be favored by smaller values of $\bar{q}_2$ for a given η (small Λ), since the transfer of large amounts of angular momentum causes the actual classical trajectory to deviate from the assumed Rutherford trajectory.

d. The Parameter ζ

Another parameter of major significance in heavy-ion Coulomb excitation is one that is characteristic of the suddenness of the interaction. The effect of a non-sudden collision upon the transfer of spin quanta is illustrated in Fig. 4. The quantum number function (final spin vs. initial orientation angle)[10,12,23] is plotted there for the case $^{136}Xe + ^{178}Hf$ (E_{Lab} = 600 MeV) both for the sudden-impact (infinite moment-of-inertia) and actual non-sudden case. The general effect is to shift the quantum number function toward smaller angles and to lower the maximum value of I_f. Thus in the sudden-impact case the function is centered at $\chi_0 = \pi/4$ because of the angular dependence of the quadrupole potential and has a maximum $I_{max} \approx 2\bar{q}_2 \approx 20$. In the real non-sudden case the maximum is shifted to $\sim 25°$ and I_{max} is reduced to ~ 14.

The effect of the non-sudden collision on the position of the maximum is virtually independent of bombarding energy, as Fig. 5 illustrates. The physical reason for this is easily seen. For higher projectile energies the collision time is shorter, but higher spins will be excited and the target will rotate faster than for lower energies. Thus the ratio between collision time and the period of rotation for the target is roughly independent of energy.[23] Therefore, the angular momentum is imparted to the target in a similar way for trajectories having different bombarding energies, but the same initial orientation χ_0.

Traditionally the adiabaticity parameter ξ_{02} defined by eq. (16-c) has been used to measure the suddenness of the reaction, but it is an energy-dependent parameter. As Massmann has suggested,[23]

a better indication of the suddenness of the reaction should be the parameter $\zeta = \xi_{02}\bar{q}_2$. From eq. (17-a), ζ is independent of energy and is characteristic only of the projectile-target system. It has a simple physical interpretation for multiple Coulomb excitation: since for collisions not too far from the sudden impact limit $\bar{q}_2 \simeq I_{max}/2 \simeq$ maximum number of E2 spin quanta transferred in the interaction, we deduce from (17-a) that ζ is the adiabaticity parameter for the lowest rotational E2 excitation multiplied by approximately the maximum number of E2 spin quanta that can be transferred in the classical interaction.

From eq. (19-c) we note that if $\zeta \simeq 0$ the target does not rotate during the collision, while if ζ is large the period of target rotation and nuclear collision may become comparable. Finally, if ζ is sufficiently large the collision becomes adiabatic and the target rotation follows the motion of the projectile, with virtually no net angular momentum transferred to the target.

4. Comparison to Quantum Mechanical Calculations

As pointed out in the previous sections, the approximations employed in the CLSM method are expected to be more valid for heavy projectiles and the excitation of large numbers of rotational states. Since this is exactly the situation for which quantum-mechanical calculations are not yet practical, this represents one of the attractive features of the method. On the other hand, this means that comparisons to quantum-mechanical calculations are easily done only for lighter systems in which the parameters η and $\bar{q}_2$ are relatively small and the CLSM method might not be expected to work very well. In fact, we have found that the CLSM gives a highly accurate description of the Coulomb excitation process even for the lightest ions. This is illustrated in Figs. 6-9 and table I for

several representative target-projectile systems. In the upper part of each figure we have plotted the amplitude and phase of the complex S-matrix for the $\ell = 0$ incident partial wave as a function of angular momentum, both for a quantum mechanical calculation and for the CLSM calculation (note that the radial scale is logarithmic). The coupled-channels quantum mechanical calculation was made with the code AROSA,[1] while all CLSM results were obtained using the integral representation of the classical-limit S-matrix (eq. (5)). In the lower part of each figure we show the relative deviation of the amplitude and the deviation of the phase of the S-matrix from the quantum mechanical calculation, both for the CLSM method and for the A-W method, with the A-W values calculated using a version of the standard Winther-deBoer code[3] and with the semiclassical amplitudes identified with the elements of the reaction matrix.[2,8] The agreement between the CLSM method and the quantum-mechanical calculation for the amplitude and the phase of the $\ell = 0$ S-matrix, even for protons, is remarkable. Furthermore, even for many of the cases where $\overline{q}_2$ and η are rather small there is clear evidence for superior accuracy of both the amplitude and the phase of the CLSM $\ell = 0$ S-matrix relative to the A-W one. As discussed in section 3, the CLSM method should improve as one goes to heavier projectiles transferring larger amounts of angular momentum.

In ref. 13) we presented comparisons of quantum mechanical probabilities to CLSM probabilities for similar systems using the simple model implied by eq. (14). The agreement was remarkably good, but there were small differences for the most forbidden transitions. From the comparison here of the amplitude and the phase of the S-matrix elements it is apparent that even these differences were not due primarily to the CLSM S-matrix elements themselves, but rather to the approximation used for the partial wave summation in the

present simple model, i.e., the reduction of the infinite sum to a single incident ℓ-wave term. While this is probably a good approximation for heavier ions (e.g. ^{40}Ar), it becomes less so for lighter projectiles.

5. The Limit $\eta \to \infty$

The Alder-Winther semiclassical method may be considered an approximation which is exact for a system in which $\eta \to \infty$ for finite $\bar{q}_2$ (i.e., $\Lambda \to 0$), since in that case the projectile wave-packet reduces to a point describing a classical Rutherford trajectory (see eq. 19-a,b). As we have noted, the A-W rotational dynamics are treated quantum-mechanically, while the CLSM method uses classical dynamics for the rotational degrees of freedom. Therefore, a comparison of the two methods in the limit $\eta \to \infty$ is instructive, since in that limit the orbital dynamics for the two methods become comparable and a direct test of the approximate CLSM model for the rotor is possible.

a. The Limit $\eta \to \infty$ and $\xi_{02} \to 0$

In this limit (corresponding to an infinite moment of inertia for $\eta \to \infty$) the A-W and quantum-mechanical models may be solved analytically for backward scattering, and the results are equivalent.[2] For the CLSM method in this limit $\bar{\chi} = \chi_0$, and the phase of eq. (6) reduces to

$$\phi' = -\frac{4}{3}\bar{q}_2 P_2(\cos\chi_0) \tag{20}$$

and from (5) and (20)

$$S_{I\leftarrow 0} = \frac{\sqrt{2I+1}}{2}\int_0^{\pi} \sin\chi_0\, P_I(\cos\chi) e^{-\frac{4}{3}i\,\bar{q}_2 P_2(\cos\chi_0)} d\chi_0$$

$$= \sqrt{2I+1}\int_0^{1} P_I(\mu) e^{-i\frac{4}{3}\bar{q}_2 P_2(\mu)} d\mu \tag{21}$$

where $\mu = \cos \chi_0$. But eq. (21) is the same analytical expression that one finds for this limit in the A-W approach (see eq. 5.11 of ref. 24). This is a very interesting result since, as has already been pointed out, the CLSM and A-W methods take qualitatively different approaches to the general scattering problem. The reason for this convergence of the two methods is not yet fully understood, but presumably is related to the disappearance, in the $\xi_{02} \to 0$ (sudden-impact) limit, of the commutation relations implied by the time-ordering operators in a Dyson series for the S-operator.†

Previously it has been shown that in this limit the A-W and USCA methods give almost exactly the same results for $\bar{q}_2 \gtrsim 2$, but there are some deviations for smaller values of $\bar{q}_2$.[10,23] Since the expression (21) may be evaluated by stationary phase methods to yield the formulas used in refs. 10) and 23), it is clear that the deviations at very small values of $\bar{q}_2$ in refs. 10) and 23) are due to approximations employed to evaluate the integral in (21), and are not due to the fundamentals of the CLSM theory. For the larger values of $\bar{q}_2$ expected in heavy-ion interactions the USCA is practically indistinguishable from the CLSM, A-W, and quantum-mechanical results in this sudden-impact limit.

b. The limit $\eta \to \infty$ for finite ξ_{02}

For the real (non-sudden) case analytical solutions are no longer possible and the A-W and CLSM probabilities must be determined numerically. In Fig. 10 we show some CLSM probabilities as a function of $1/\eta$ for a representative heavy-ion system. The curves were obtained by keeping $\bar{q}_2$ and ξ_{02} fixed at their relistic values while varying η in eqs. (19), where $\Lambda = \bar{q}_2/\eta$ and $\zeta = \xi_{02}\bar{q}_2$. The

---

†See ref. 2), pp. 21 f.f. We are indebted to Dr. R. A. Malfliet for this suggestion.

behavior is seen to be rather linear in $1/\eta$ for this region, though there is some curvature in several cases.

Normally in the A-W method the effect of finite energy transfer in an inelastic event is approximated by employing a trajectory symmetrized over translational energies in the entrance and exit channels. A symmetrization of this nature is superfluous in the CLSM method since the projectile motion is governed by exact classical dynamics during the entire scattering process. It is clear that in the limit $\eta \to \infty$ the CLSM results should be compared to the A-W results using unsymmetrized orbits. The unsymmetrized A-W probabilities, calculated using a Winther-deBoer code modified such that the projectile energy remains equal to the incident energy for all transitions, are shown in Table II and displayed on the left axis of Fig. 10 as dark circles. The CLSM results extrapolated for $\eta \to \infty$ are shown in Table II for all transitions and in Fig. 10 for those transitions in which the η-dependence is strongest. The agreement between the CLSM results and the A-W results (which are exact in this limit) is excellent. In particular we note that for the 14^+ and 16^+ states the CLSM probabilities change by 50-100% in going from the realistic value of $\eta = 127$ to $\eta = \infty$, for which they yield almost exactly the A-W result. Since in this limit the treatment of the orbital dynamics in the A-W and CLSM methods are equivalent, this result leads to an important conclusion: the treatment of the internal rotational degrees of freedom by classical dynamics plus the superposition principle and quantized boundary conditions is able to quantitatively reproduce the exact quantal treatment of those degrees of freedom for heavy-ion scattering from deformed targets. This suggests that in the A-W and the CLSM methods any significant discrepancy with quantum mechanics for heavy-ion scattering is a function of the orbital dynamics. Since the CLSM method employs exact classical orbital dynamics and the A-W method uses approximate classical orbital dynamics, this suggests that for heavy ions and deformed targets the CLSM method should be more accurate than the semiclassical A-W method.

This conclusion is strengthened by considering the symmetrized A-W results for the same problem. These are shown in Table II and plotted on the left axis of Fig. 10 as open squares. In some cases the energy symmetrization lowers the A-W results relative to the unsymmetrized calculation and in some cases it raises it. In every case the introduction of energy-symmetrized orbits changes the A-W probabilities in the direction of the CLSM results at the realistic value of $\eta = 127$ (the dashed vertical line in Fig. 10). This is exactly the behavior one expects if the differences between the CLSM and A-W results at the realistic η are due to approximate orbital dynamics in the latter method, since this symmetrization is introduced in the A-W method precisely for the reason of improving the approximate classical orbit.†

By this argument the discrepancy remaining between CLSM and A-W probabilities following the A-W energy symmetrization is due primarily to neglecting the coupling of projectile orbital angular momentum to internal rotational modes of the target in the scattering process. This suggests that a symmetrization with respect to angular momentum transfer in addition to energy transfer could lead to an improvement in the A-W method. These symmetrizations are being investigated.[8)]

6. Comparison of CLSM and A-W Probabilities for Heavy Systems

In Fig. 11 we show calculated excitation probabilities for head-on collisions in several representative heavy-ion systems using CLSM and A-W methods. Over all, the calculations are in rather good agreement with each other, but there are some systematic differences for the highest

---

†This symmetrization is given theoretical foundation by considering WKB approximations to first and second-order quantum-mechanical perturbation theory.[2)]

spins. The preceding arguments suggest that these differences are primarily due to the approximate classical orbital dynamics of the A-W method. If those arguments are correct, the differences between the CLSM and A-W curves in Fig. 11 represent the orbital dynamics component of the "quantal" correction to semiclassical (A-W) Coulomb excitation theory. This component of the correction (which is independent of $\hbar$) is expected to be dominant for Coulomb excitation with heavy ions, since explicitly $\hbar$-dependent effects should become vanishingly small for semiclassical calculations on systems with very large values of η.

In Fig. 11 there is a division of the excitation probabilities into two distinct regions of behavior: the classically accessible region, characterized by oscillatory structure; and the classically forbidden region, marked by a sharp fall-off of the excitation probabilities with spin. For the CLSM method in the saddle-point limit there is a clear conceptual distinction between these two regions. In the classically accessible region two (real) initial orientations contribute saddle points to the S-matrix (eq. 10 and Fig. 2-a) and the excitation probability receives contributions from two terms and their interference term (see eq. 15-a), hence the oscillatory structure. For the classically forbidden region the topology of the integrand in eq. (9) is such that only one saddle point (complex orientation angle) contributes to the probability amplitude (Fig. 2-b), and it is exponentially damped due to penetration of the projectile into regions inaccessible to classical dynamics with real trajectories (eq. 15-b). Hence the forbidden transition probabilities exhibit no oscillations but instead decrease rapidly with increasing spin.

In the classically accessible regions of Fig. 11, the deviations of the A-W calculations from the CLSM ones are generally small and exhibit

positive and negative fluctuations. For the classically forbidden regions the differences are larger and the CLSM probabilities are smaller than the corresponding A-W ones.

From eq. (19-b) and the preceding discussions we note that the essential difference between trajectories in the A-W and CLSM approaches is the neglect of the monopole-quadrupole coupling effect on the projectile motion in the former method. For the region of orientation space in which the maximum of the quantum-number function occurs for a quadrupole potential ($\chi_0 \leq \pi/4$) the monopole-quadrupole interaction is repulsive (see Figs. 4-5 and eq. 19-b). Therefore, for those trajectories leading to the highest spins, the projectile penetrates closer to the target nucleus on the approximate A-W hyperbolic trajectory than it does on the exact trajectory of the CLSM, if we confine ourselves to real turning points and to reactions which are not too adiabatic. In the CLSM the projectile may, of course, penetrate inside the classical turning point--that is the significance of the uncertainty principle which in this context allows complex trajectories leading to forbidden states--but in so doing, the momentum, and hence all variables in the coupled equations of motion, become complex. This damps the probability by giving rise to an imaginary component in the phase (cf. eq. 15-b). As a consequence there is generally less monopole-quadrupole interaction on the exact trajectory than on the hyperbolic one, and on the average, fewer spin quanta will be exchanged on the exact trajectory than on the hyperbolic one. Therefore excitation of higher-spin states will be over-emphasized and, since the unitary S-matrix conserves probability, excitation of lower-spin states will be under-emphasized in the A-W calculation with hyperbolic trajectories.

Both effects are seen in Fig. 11. For the high-spin (classically forbidden) transitions the CLSM probabilities lie uniformly lower than those from the A-W calculation. The picture is more complicated for the low-spin (classically allowed) states because, in classical trajectory terminology, two initial orientations contribute to the probability amplitude in that case, and cognizance must be taken of the interference term between these contributions in the expression for the probability (cf. eq. 15-a). Thus, although the summed probabilities for all the classically allowed states are slightly higher for the CLSM calculations than for the A-W ones, the probability for a particular state may be either increased or decreased by the inclusion of exact orbital dynamics. Which direction will be dictated by two considerations: 1) the effect of the altered trajectories on the average number of spin quanta transferred (which affects the P_k of eq. (11)), and 2) the effect of the altered trajectories on the real phase difference in the interference term of eq. 15-a.

Finally, we note that the relatively good agreement between the CLSM and A-W calculations except at the highest spins is consistent with recent experimental evidence setting upper limits on any corrections to A-W semiclassical calculations.[25,26] For example, an extensive comparison of transition probabilities for states in ^{232}Th determined by various Doppler-shift lifetime methods and by multiple Coulomb excitation places an upper limit of 15-20% on the correction to the A-W probabilities for $I^{\pi} \leq 16^{+}$ with 623-MeV ^{136}Xe projectiles.[25] This upper limit is consistent with the indicated differences in Fig. 11.

7. Conclusions

The classical limit of the quantum mechanical S-matrix for multiple Coulomb excitation has been investigated by direct numerical evaluation of the S-matrix in an integral representation, and by employing complex classical trajectories in a saddle point approximation to the integral S-matrix. We have demonstrated that this method is capable of reproducing both the amplitude and the phase of the quantum-mechanical S-matrix elements, even for projectiles as light as protons. Because the dynamics are completely classical the equations of motion, parametrized in terms of a set of dimensionless variables, yield valuable insight into the nature of the orbital dynamics in semiclassical approaches.

From the above considerations and from examination of the limit $\eta \to \infty$, we find evidence that the "quantal" correction to the Alder-Winther theory for heavy ions is dominated by a component which is independent of $\hbar$. This component is shown to arise from the approximate classical orbital dynamics in the Alder-Winther theory, rather than from true quantum-dynamical effects. Therefore, it is suggested that the present dynamically exact classical-limit S-matrix approach, or an improved symmetrization of the orbitals in the Alder-Winther method, should yield highly accurate results for heavy-ion multiple Coulomb excitation. Calculations performed for several representative heavy-ion systems indicate that this correction due to orbital dynamics for the Alder-Winther probabilities is usually small ($\lesssim 20\%$) for states accessible with current experimental techniques. This is consistent with recent experimental results setting an upper limit on the magnitude of this effect.

For historical reasons, much of the discussion here has been in terms of quantal corrections to earlier semiclassical calculations. Therefore, it is important to reiterate that the classical limit S-matrix method represents not a mere correction but an independent, self-contained approach to heavy-ion scattering problems. The essential practical limitations of the present simple model are its restriction to zero impact parameter and the omission of vibrational and rotational-vibration channels in the excitation process. These restrictions are removable in principle, and work is currently in progress to do so.[14,18] The extension to all impact parameters for the classically allowed transitions in the general case,[18] and to all transitions for the sudden-impact limit has been accomplished,[14] but a number of obstacles have thus far precluded a completely general solution. The accuracy exhibited by the method in the simple model used here suggests that the general solution will be of great use when it is obtained.

The fact that this method requires a classical model for the nuclear excited states and excitation matrix elements has good and bad aspects. On the one hand, other semiclassical methods should be more versatile in the treatment of general problems since they employ model-independent matrix elements rather than specific classical models. However, many nuclear systems (e.g. highly deformed nuclei) can be approximated quite nicely by simple rotation-vibration models. In such cases the CLSM approach has a clear conceptual advantage because it leads to simple and suggestive pictures for the excitation process. In addition, the CLSM method may exhibit superior accuracy relative to other semiclassical methods if dynamical approximations in other methods are more important than the model approximations in the CLSM.

As discussed elsewhere,[12] the methods used here may be extended to describe the exact classical dynamics of a projectile moving in a deformed

complex nuclear potential. Thus, a unified theory of interaction at barrier and sub-barrier energies is possible which includes on an equal footing the effects of all contributing components in the electric multipole field, and the real and imaginary parts of a complex nuclear potential.

For heavy-ion interactions on highly deformed nuclei at near-barrier energies dynamical approximations may become critical because 1) relative to Coulomb excitation the real interaction may be expected to be sharply varying both radially and in the target-nucleus orientation angle, 2) large angular momentum and energy transfers may be involved, and 3) the imaginary potential may distort the orbit itself in addition to absorbing particle flux. Under these conditions the exact classical dynamics of the CLSM method should become increasingly important.

From these considerations it seems apparent that CLSM and other semiclassical methods will be useful as complementary techniques in the study of heavy-ion scattering. The discussion here and in ref. 8-b) should serve to clarify which situations are most appropriate for a classical-limit type approach, and which for one of the other semiclassical methods. Obviously, a tractable quantum mechanical calculation for heavy-ion scattering from deformed nuclei is desirable. Even if such calculations become possible, however, classical-limit and semiclassical methods may still be expected to retain their conceptual importance for heavy-ion scattering.

References

1) F. Roesel, J. X. Saladin, and K. Alder, Comp. Phys. Comm. 8 (1974) 35.

2) K. Alder and A. Winther, "Electromagnetic Excitation," North Holland, 1975.

3) A. Winther and J. deBoer in "Coulomb Excitation," by K. Alder and A. Winther ed., Academic Press, New York, p. 303.

4) K. Alder, R. Morf, and F. Roesel, Phys. Lett. 32B (1970) 645.

5) K. Alder, F. Roesel, and R. Morf, Nucl Phys. A186 (1972) 449.

6) K. Alder, Heavy Ion Summer Study, Oak Ridge National Laboratory, Oak Ridge, Tennessee, 1974.

7) K. Alder, F. Roesel, and J. X. Saladin, in Proceedings of the International Conference on Reactions between Complex Nuclei, Nashville, Tenn. 10-14 June, 1974, edited by R. L. Robinson, F. K. McGowan, J. M. Ball, and J. H. Hamilton (North-Holland, Amsterdam/American Elsevier, New York, 1974), Vol. II.

8) J. deBoer, H. Massmann, and A. Winther, Contribution to International Workshop III, on Gross Properties of Nuclei and Nuclear Excitations, Hirschegg, Austria, Jan. 13-18, 1975 (unpublished); and J. DeBoer, D. Dannhäuser, H. Massmann, F. Roesel, and A. Winther, to be published.

9) S. Levit, U. Smilansky, and D. Pelte, Phys. Lett. 53B (1974) 39.

10) H. Massmann and J. O. Rasmussen, Nucl. Phys. A243 (1975) 155.

11) See W. H. Miller, Advances in Chemical Physics, 25 (1974) 69, and references therein.

12) M. W. Guidry, H. Massmann, R. Donangelo, and J. O. Rasmussen, Nucl. Phys. A274 (1976) 183.

13) R. Donangelo, M. W. Guidry, J. P. Boisson, and J. O. Rasmussen, Phys. Lett. 64B (1976) 377.

14) R. Donangelo, Ph.D. thesis, University of California, Berkeley (1977), unpublished.

15) T. Koeling and R. A Malfliet, Phys. Reports 22C (1975) 182.

16) J. Knoll and R. Schaeffer, Phys. Lett. 52B (1974) 131.

17) J. Knoll and R. Schaeffer, Annals of Phys. 97 (1976) 307.

18) P. Fröbrich, Q. K. K. Liu, and K. Möhring, to be published, and 4° Session D'Etudes Biennale de Physique Nucleaire, La Toussuire, France (1977).

19) M. S. Child, "Molecular Collision Theory," North Holland, 1975.

20) W. H. Miller, J. Chem. Phys. 53 (1970) 1949.

21) W. H. Wong and R. A. Marcus, J. Chem. Phys. 55 (1971) 5663.

22) J. N. L. Connor and R. A. Marcus, J. Chem. Phys. 55 (1971) 5636.

23) H. Massmann, Ph.D. Thesis, University of California, Berkeley (1975), unpublished. (LBL-4316)

24) K. Alder and A. Winther, Kgl. Dansk. Viden. Selsk., Mat.-Fys. Medd. 32, No. 8 (1960).

25) M. W. Guidry, P. A. Butler, P. Colombani, I. Y. Lee, D. Ward, R. M. Diamond, F. S. Stephens, E. Eichler, N. R. Johnson, and R. Sturm, Nucl. Phys. A266 (1976) 228.

26) D. Ward, P. Colombani, I. Y. Lee, P. A. Butler, R. S. Simon, R. M. Diamond, and F. S. Stephens, Nucl. Phys. A266 (1976) 194.

TABLE I. Amplitude and phase of the $\ell = 0$ S-matrix element.

System	E_{LAB} (MeV)	Spin	CLSM[a]		Quantum-Mechanical[b]		Alder-Winther[c]	
			Amplitude	Phase (radian)	Amplitude	Phase (radian)	Amplitude	Phase (radian)
$^{1}H + ^{168}Er$	7	0	0.991	0.006	0.994	0.005	0.996	0.001
		2	0.134	4.670	0.113	4.680	0.135	4.670
$^{2}H + ^{168}Er$	7	0	.9824	0.010	.9859	0.009	.9824	0.003
		2	.1868	4.654	.1671	4.664	.1863	4.653
		4	.0081	3.216	.0082	3.145	.0143	3.140
$^{4}He + ^{168}Er$	14	0	.9344	0.028	.9397	0.027	.9339	0.014
		2	.3532	4.606	.3390	4.615	.3532	4.599
		4	.0469	3.094	.0441	3.080	.0544	3.067
$^{10}Be + ^{168}Er$	45	0	.3424	1.027	.3472	0.988	.3296	0.951
		2	.6911	4.517	.7009	4.513	.6613	4.378
		4	.5828	2.736	.5704	2.752	.5954	2.604
		6	.2488	1.153	.2421	1.169	.2976	1.024
		8	.0594	5.960	.0635	5.943	.1013	5.809
		10	.0093	4.373	.0110	4.480	.0256	4.368

Table I Footnotes

a) Calculations performed using integral method. See caption of of Figs. 6-9 for details.

b) Obtained from coupled-channels code AROSA.[1)]

c) Obtained from semiclassical Winther-deBoer code.[3)]

TABLE II. Excitation probabilities as a function of $1/\eta$ for a characteristic heavy-ion system.[a)]

Spin	CLSM ($\eta \to \infty$) (parabolic extrapolation)	Symmetrized Winther-deBoer	Unsymmetrized Winther-deBoer
0	0.0739	0.0739	0.0738
2	0.1684	0.1713	0.1707
4	0.0608	0.0579	0.0580
6	0.1749	0.1803	0.1784
8	0.2944	0.2937	0.2926
10	0.1688	0.1660	0.1676
12	0.0489	0.0477	0.0492
14	0.0088	0.0082	0.0087
16	0.0010	0.0009	0.0010

a) For this calculation $Q_0^{(2)} = 11.12$ eb, $Q_0^{(4)} = 0$, and $E_{2+} = 0.0449$ MeV, corresponding to $^{40}Ar + ^{238}U$ at $E_{Lab} = 170$ MeV. The realistic η for this case is 126.5.

Figure Captions

1. The coordinate system for the projectile and rotor in the simple zero impact parameter case.
2. The position of the saddle points for Coulomb excitation in the zero-impact parameter case. Part (a) is for classically allowed transitions, with two real saddle points. Part (b) represents forbidden transitions, to which only one of the complex conjugate imaginary saddle points contributes. The solid line represents the integration path for the integral method (real axis), and the dashed path indicates the steepest-decent integration path employed in the saddle-point method. The integrals are equivalent if the region between the paths contains no poles. In the case of a complex potential the clear distinction between forbidden and allowed states is erased and all saddle points are complex.[12)]
3. A schematic diagram of the relationships among various methods used in this paper. A more detailed diagram may be found in ref. 8-b).
4. The quantum-number function (final spin vs. initial orientation χ_0 for $^{136}Xe + ^{178}Hf$. The quantum-number function in the sudden impact limit is represented by a dashed line. Because the parameter $\zeta = \xi_{02} q_2$ is relatively large for this system the function is shifted considerably downward and toward lower angles in the realistic non-sudden case, typical of a highly adiabatic interaction.
5. The quantum-number function for two different heavy-ion systems at various incident energies. The position of the maximum is seen to be independent of energy for each system. The $^{136}Xe + ^{178}Hf$ curves are

shifted farther to the left because it is more adiabatic (larger ζ) than the $^{40}Ar + ^{238}U$ system.

6.-9. (a) The complex $\ell = 0$ S-matrix in a polar plot for Coulomb excitation of the ground band in ^{168}Er by several particles. The radial scale is logarithmic. The classical limit S-matrix calculation (CLSM) is in excellent agreement with an exact quantum-mechanical calculation. All CLSM calculations used the integral method. We have used the chemist's terminology (e.g., ref. 10) in calling this the S-matrix. This same quantity is often termed the R-matrix in Coulomb excitation.[2] The differences here are semantic only since the R- and S-matrix elements are related by a Coulomb phase. All projectiles were assumed spherical with no internal structure. ^{10}Be was chosen for the theory-theory comparison because the resultant value of η is near the upper limit for the quantum-mechanical code which we employed.

(b) The difference in phase between the exact quantum mechanical $\ell = 0$ S-matrix and the classical-limit S-matrix (CLSM) and Alder-Winther (A-W) semiclassical calculations.

(c) The fractional difference in amplitude between the $\ell = 0$ quantum-mechanical S-matrix and the classical-limit S-matrix (CLSM) and Alder-Winther (A-W) ones.

10. Excitation probabilities as a function of $1/\eta$ for a representative heavy-ion system. These calculations were performed with the integral method but the saddle-point method gives similar results. The results of a symmetrized (squares) and unsymmetrized (solid circles) Winther-deBoer calculation, and the extrapolated CLSM results (open circles) are shown on the left axis. As discussed in the text, the fact that the CLSM probabilities extrapolate to the

unsymmetrized Winther-deBoer results at $\eta = \infty$ strongly suggests that any significant differences between the A-W and CLSM methods for heavy ions is due to the approximate orbital dynamics of the former. As further discussed in the text, the fact that the symmetrized Winther-deBoer results always lie closer than the unsymmetrized results to the CLSM probability at the realistic value of $\eta = 127$ (dashed vertical line) also supports this conclusion.

11. Excitation probabilities for $\ell = 0$ in several representative heavy-ion systems. The A-W probabilities were calculated using a standard Winther-deBoer code. For the lightest 3 projectiles the CLSM probabilities were calculated using the integral method. For the heaviest projectile the USCA with complex trajectories was used because of numerical problems in the integral method as presently formulated for highly adiabatic systems (large values of ζ).[14] The division between classically allowed and forbidden transitions is clearly seen, as is the effect of the adiabaticity on the final angular momentum for the very heavy projectiles. As discussed in the text, we suggest that the differences between the A-W and CLSM results is a consequence of the approximate orbital dynamics in the former.

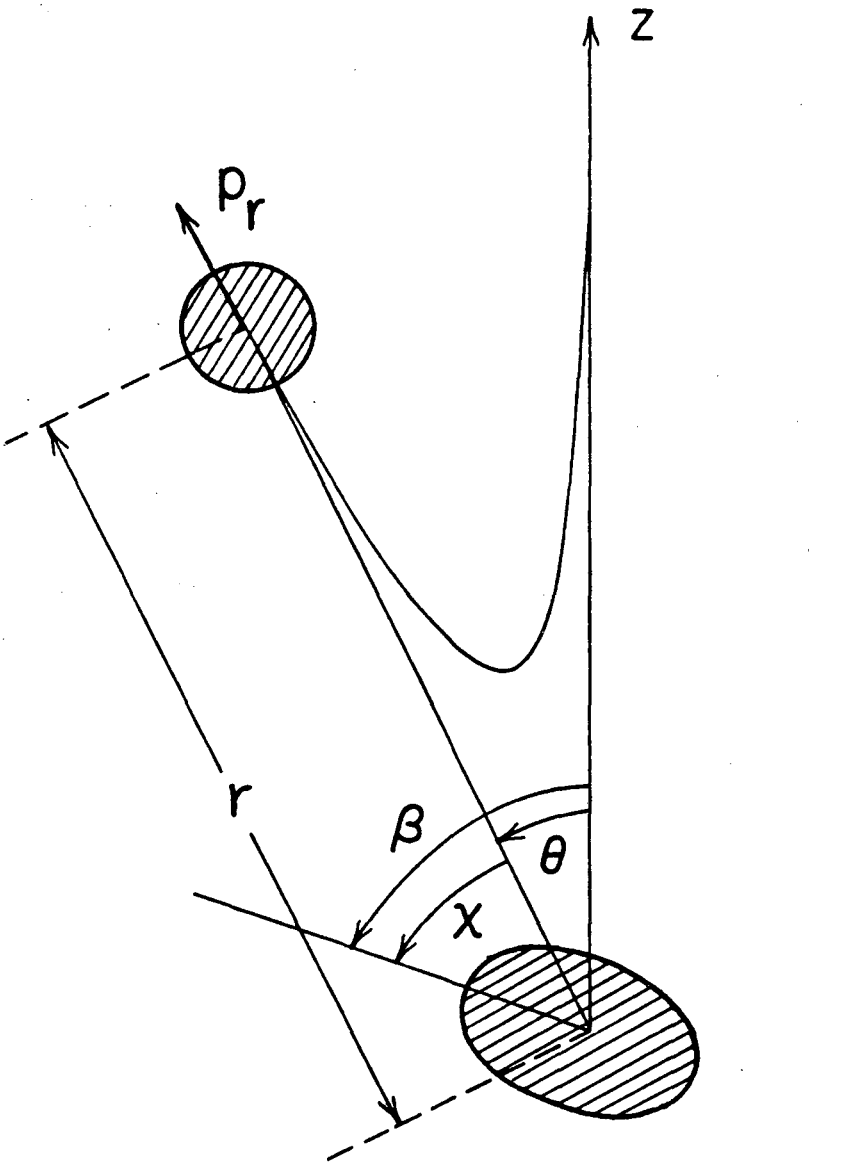

XBL7411-8214

Fig. 1

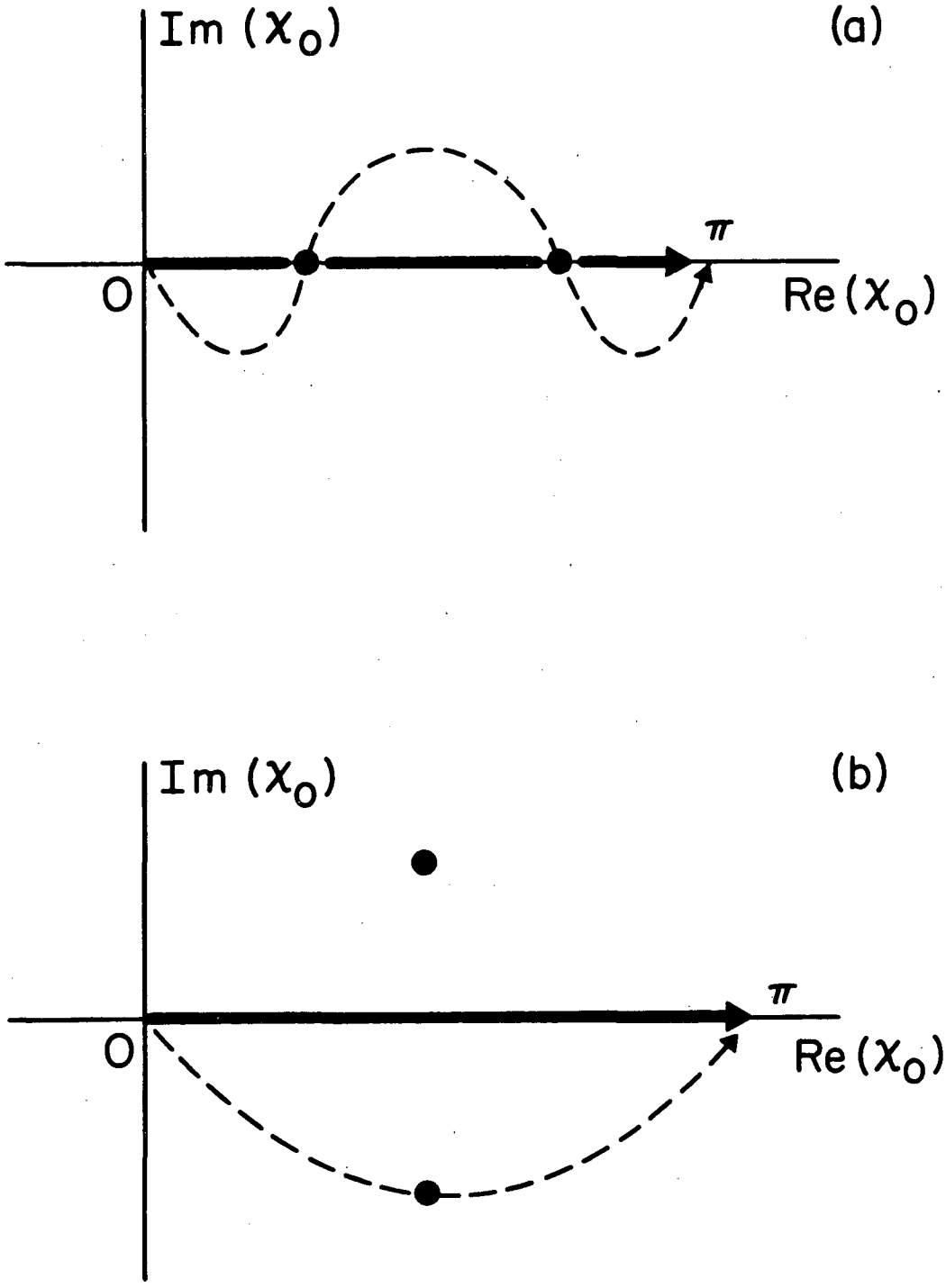

XBL 777-9485

Fig. 2

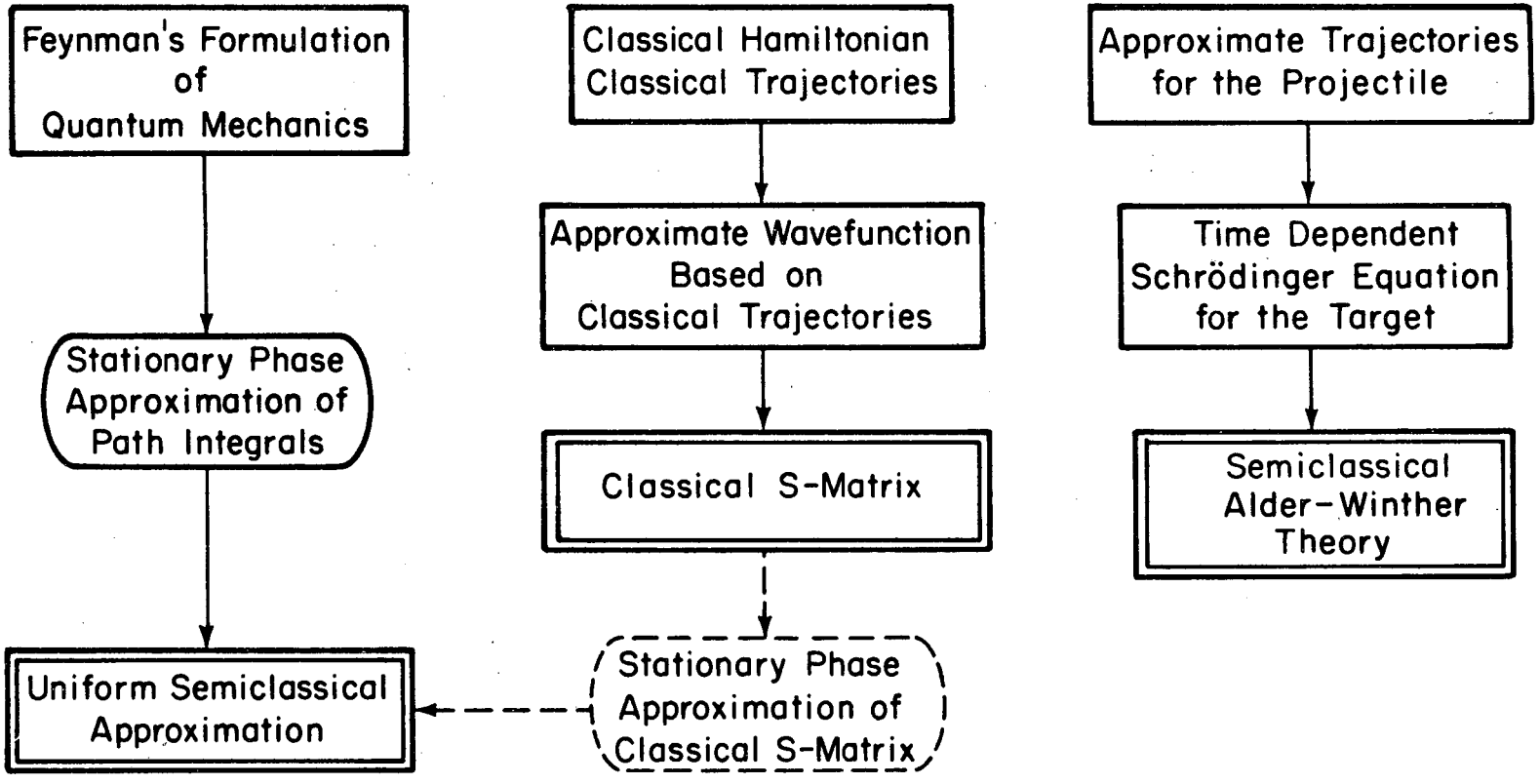

XBL 775-8584

Fig. 3

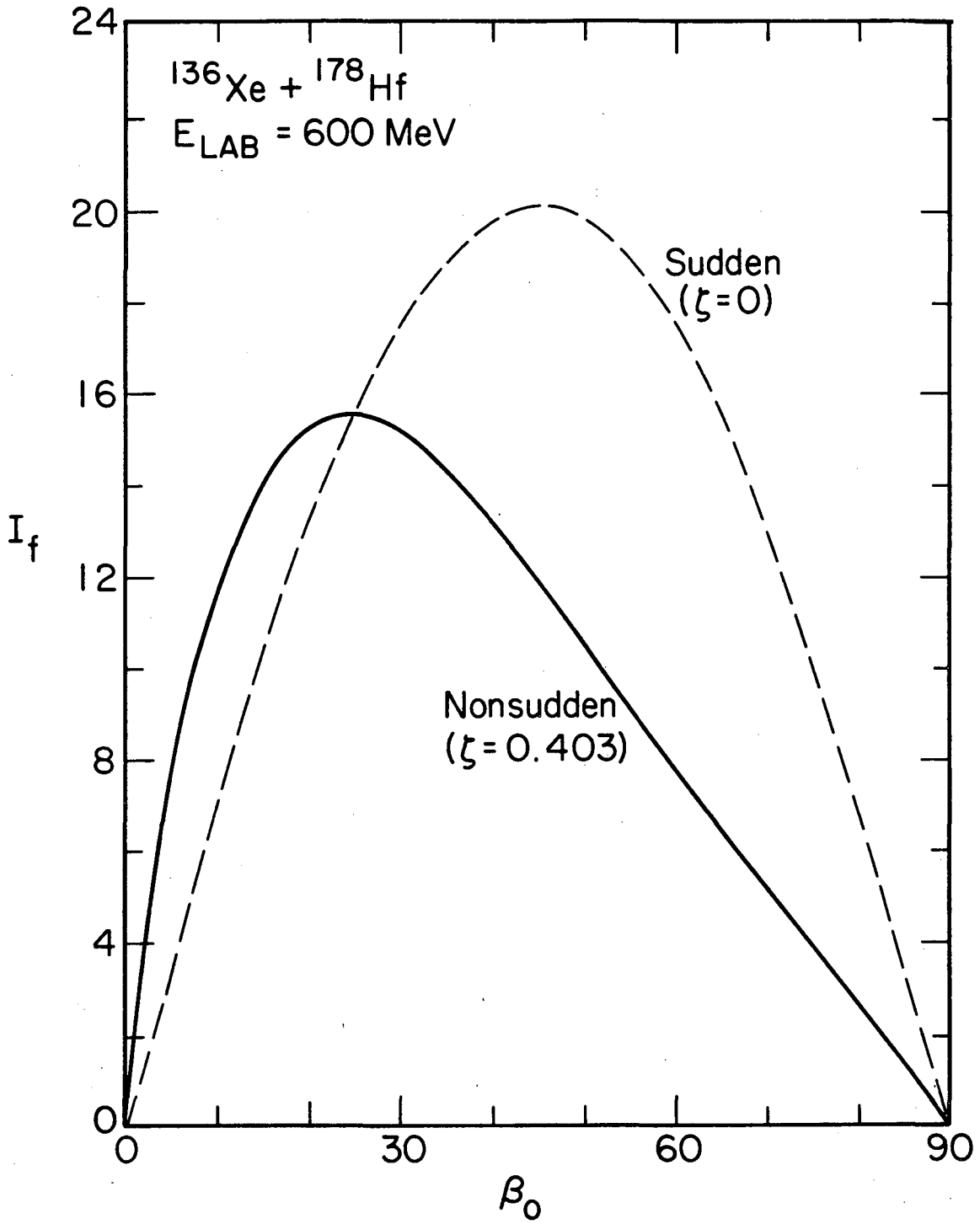

Fig. 4

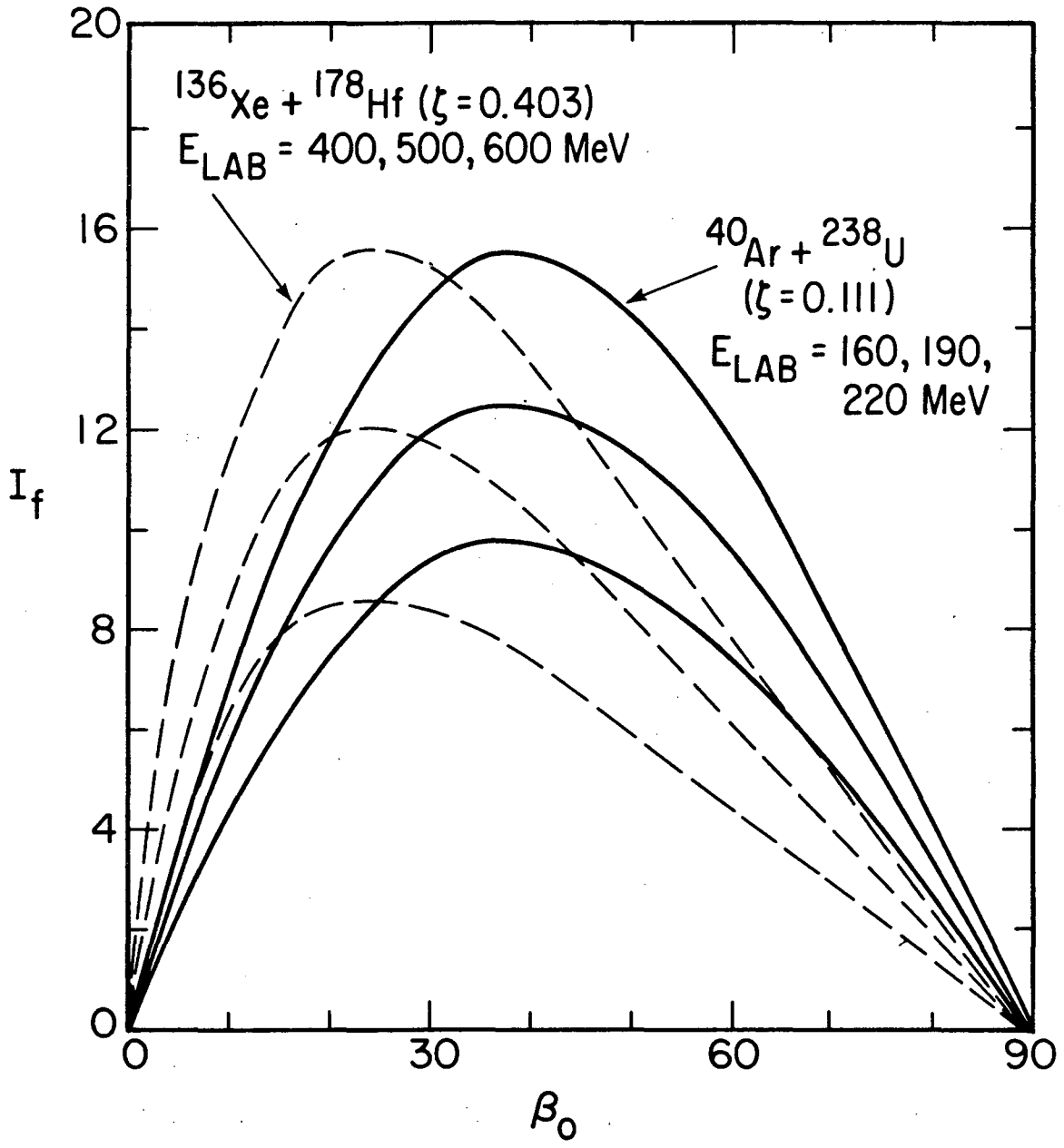
20
16
12
8
4
0
I_f
0
30
60
90
β_0
$^{136}Xe + ^{178}Hf$ ($\zeta = 0.403$)
E_{LAB} = 400, 500, 600 MeV
$^{40}Ar + ^{238}U$
($\zeta = 0.111$)
E_{LAB} = 160, 190, 220 MeV
XBL 763-787

Fig. 5

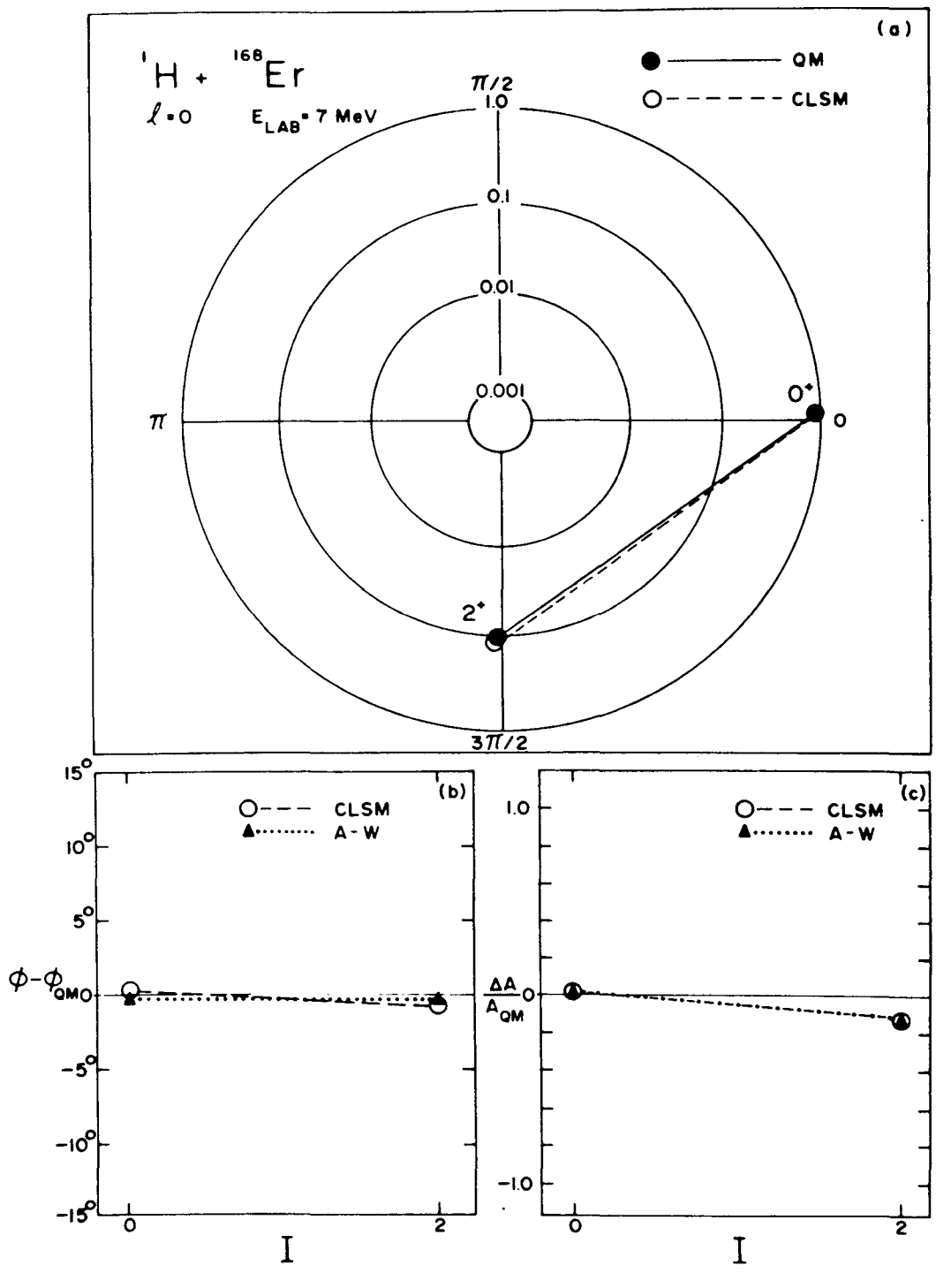

Fig. 6

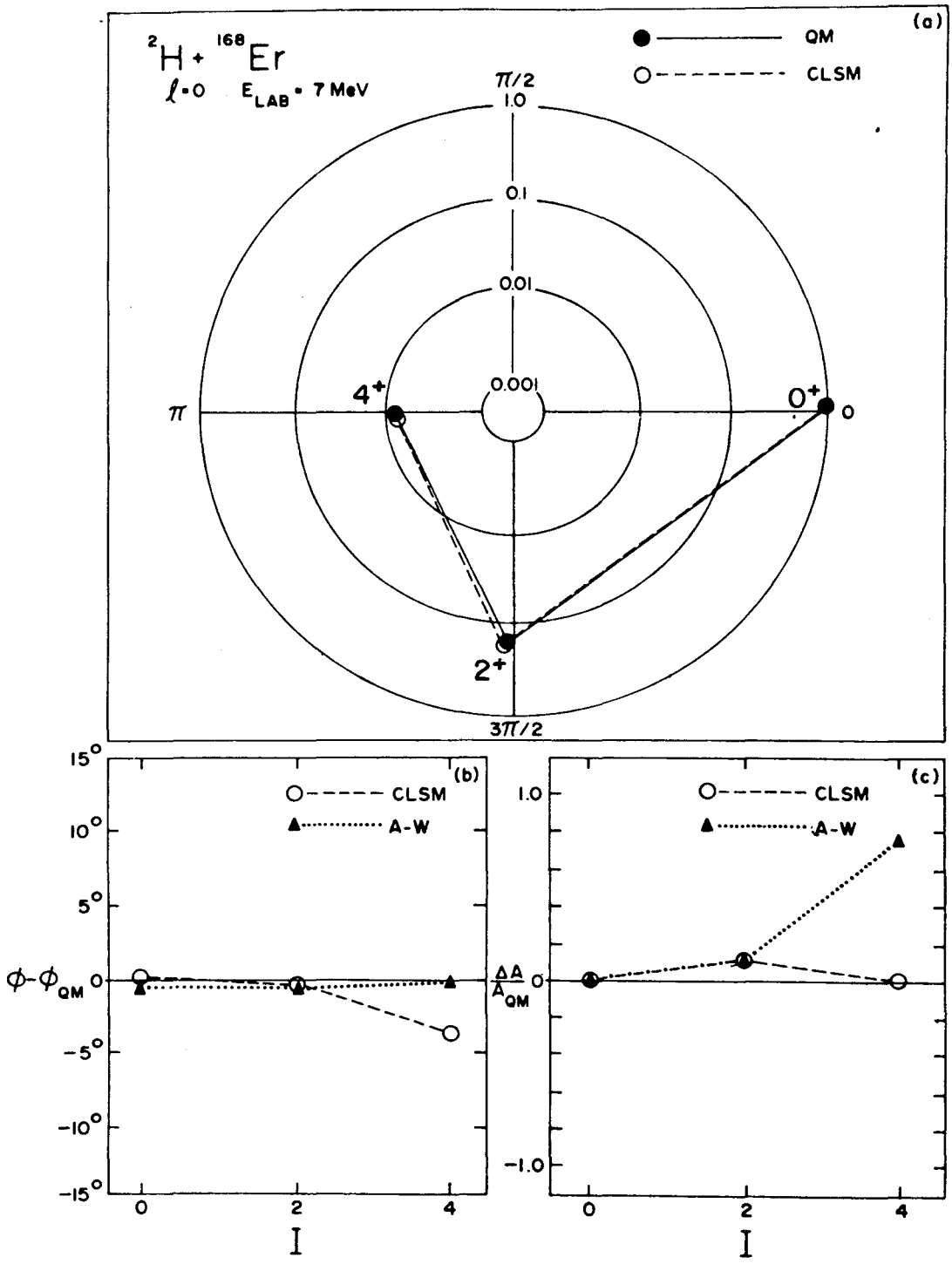
(a)
$^{2}H + ^{168}Er$
$\ell = 0$ $E_{LAB} = 7$ MeV
QM
CLSM
$\pi/2$
1.0
0.1
0.01
0.001
π
4^+
0^+
0
2^+
$3\pi/2$
(b)
CLSM
A-W
15°
10°
5°
$\phi - \phi_{QM}$ 0
-5°
-10°
-15°
0
2
4
I
(c)
CLSM
A-W
1.0
$\frac{\Delta A}{A_{QM}}$ 0
-1.0
0
2
4
I
XBL 774-8304

Fig. 7

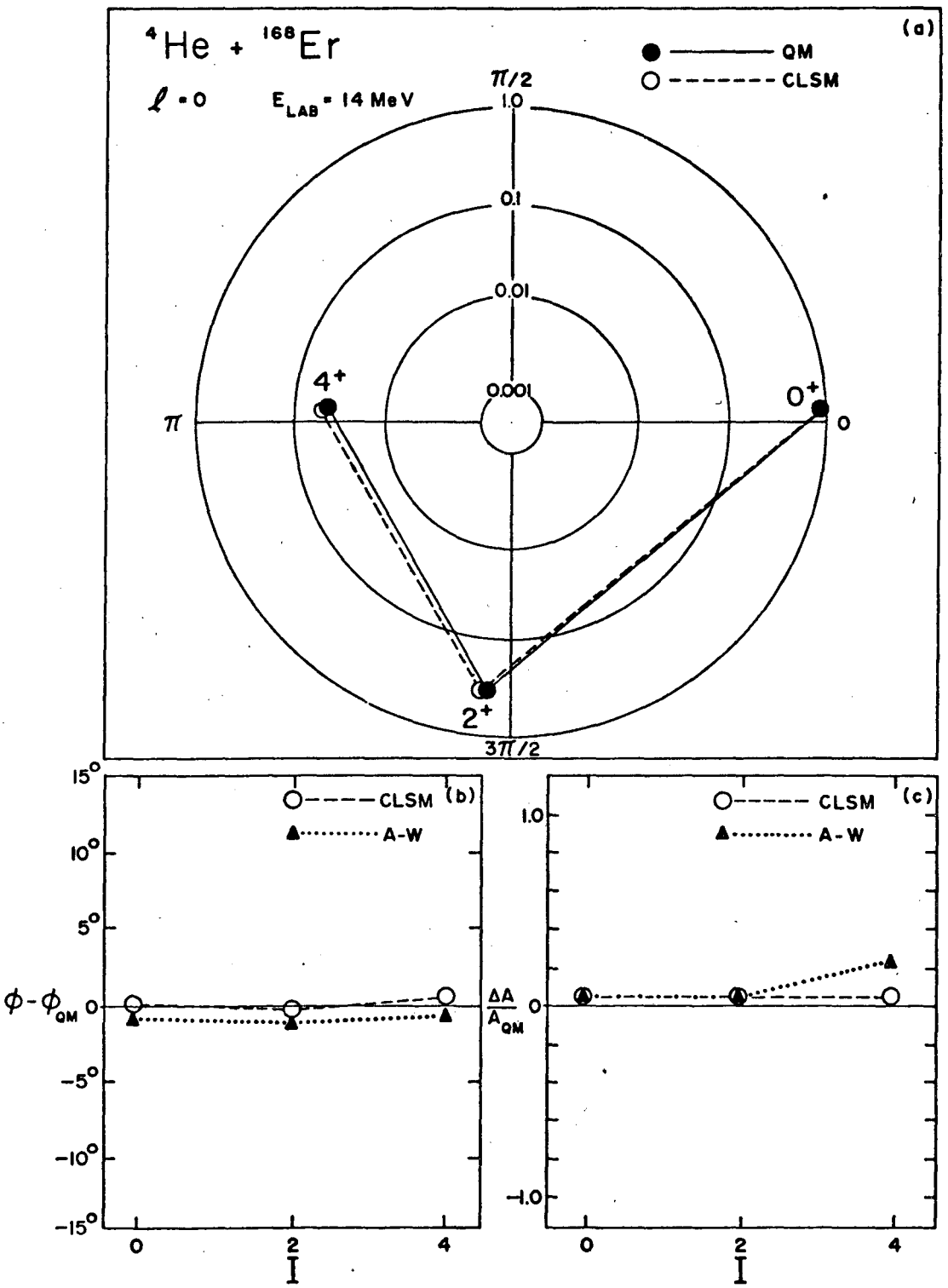

XBL 774-8301

Fig. 8

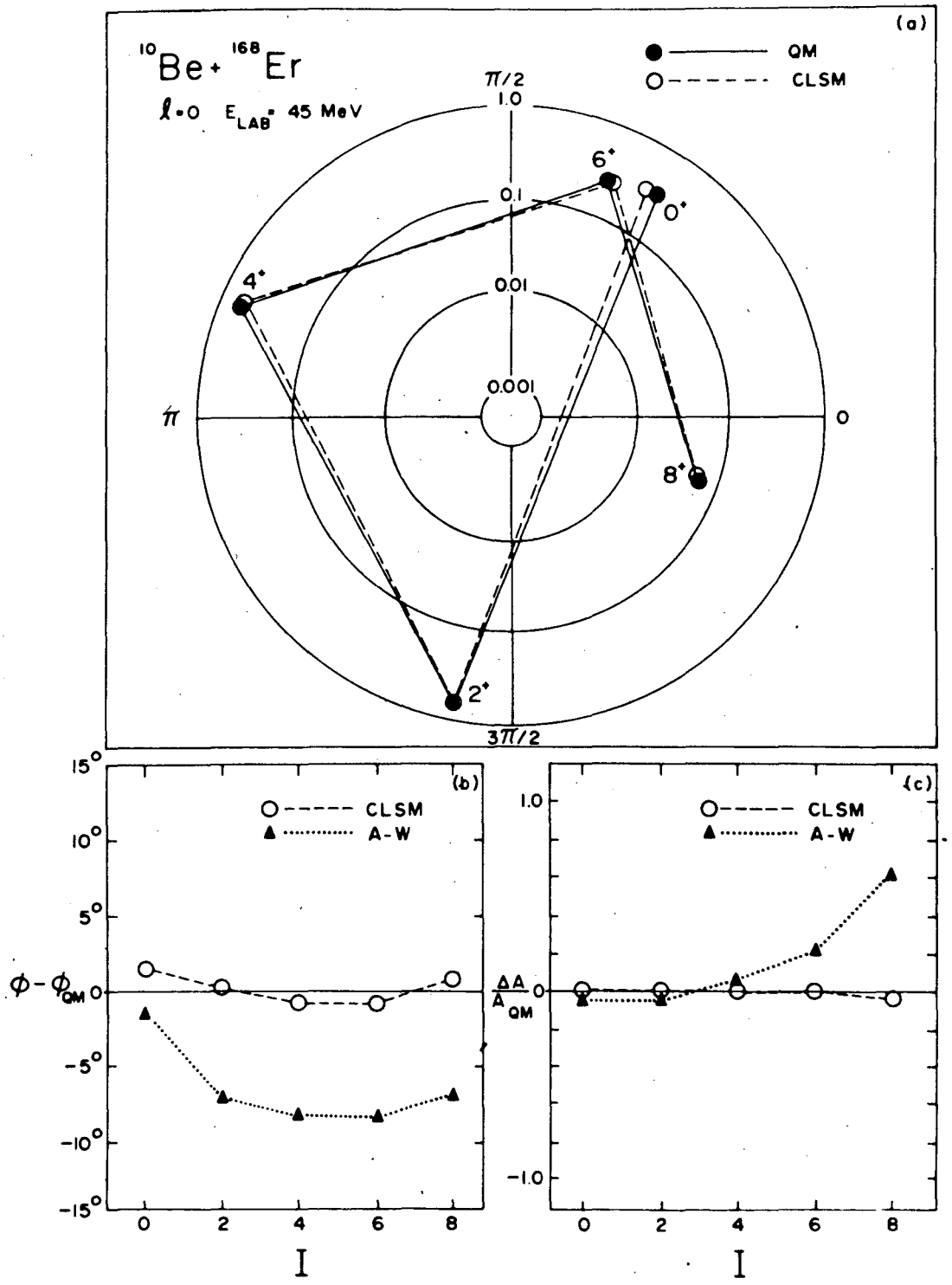

XBL 774-8302

Fig. 9

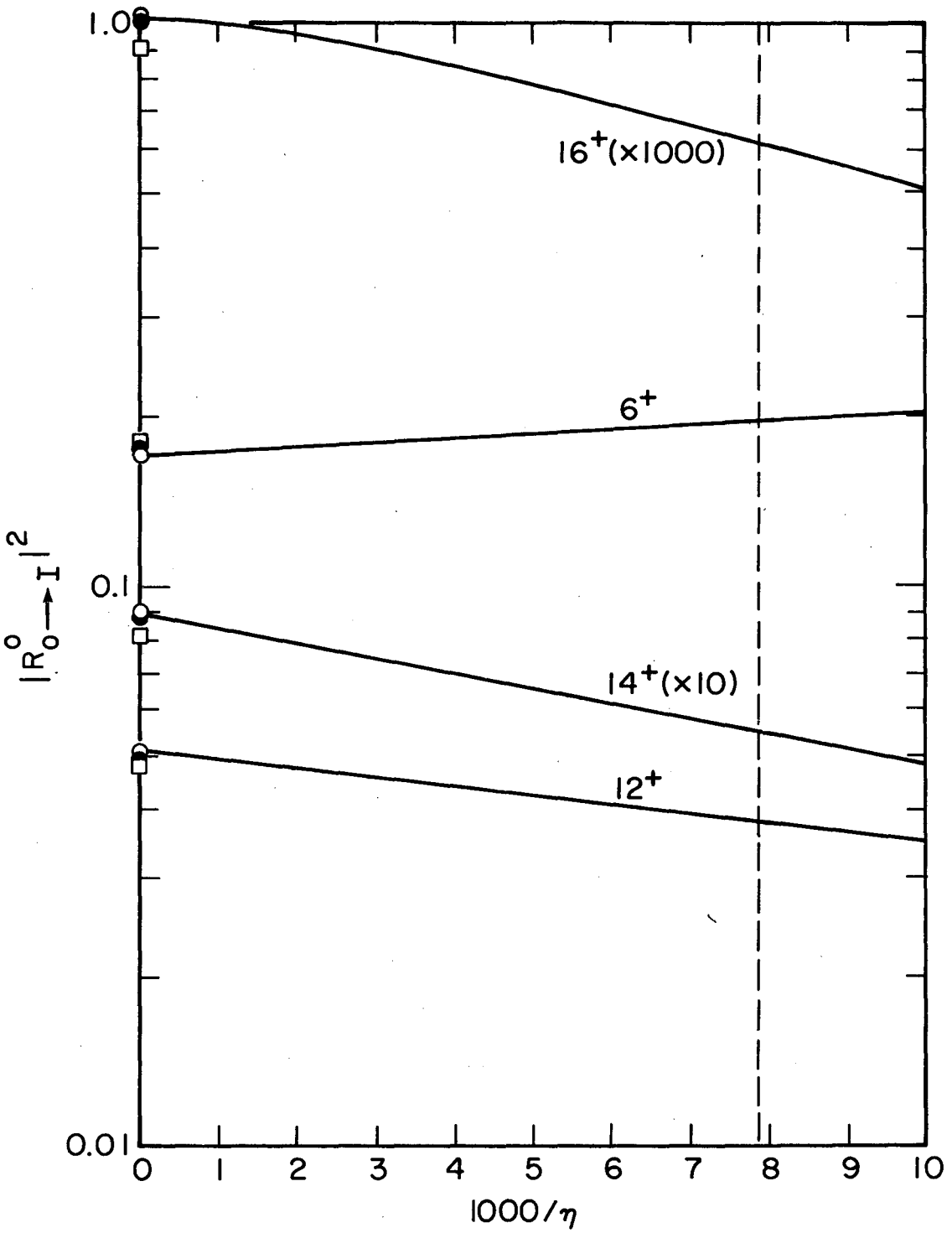

XBL 774-8291

Fig. 10

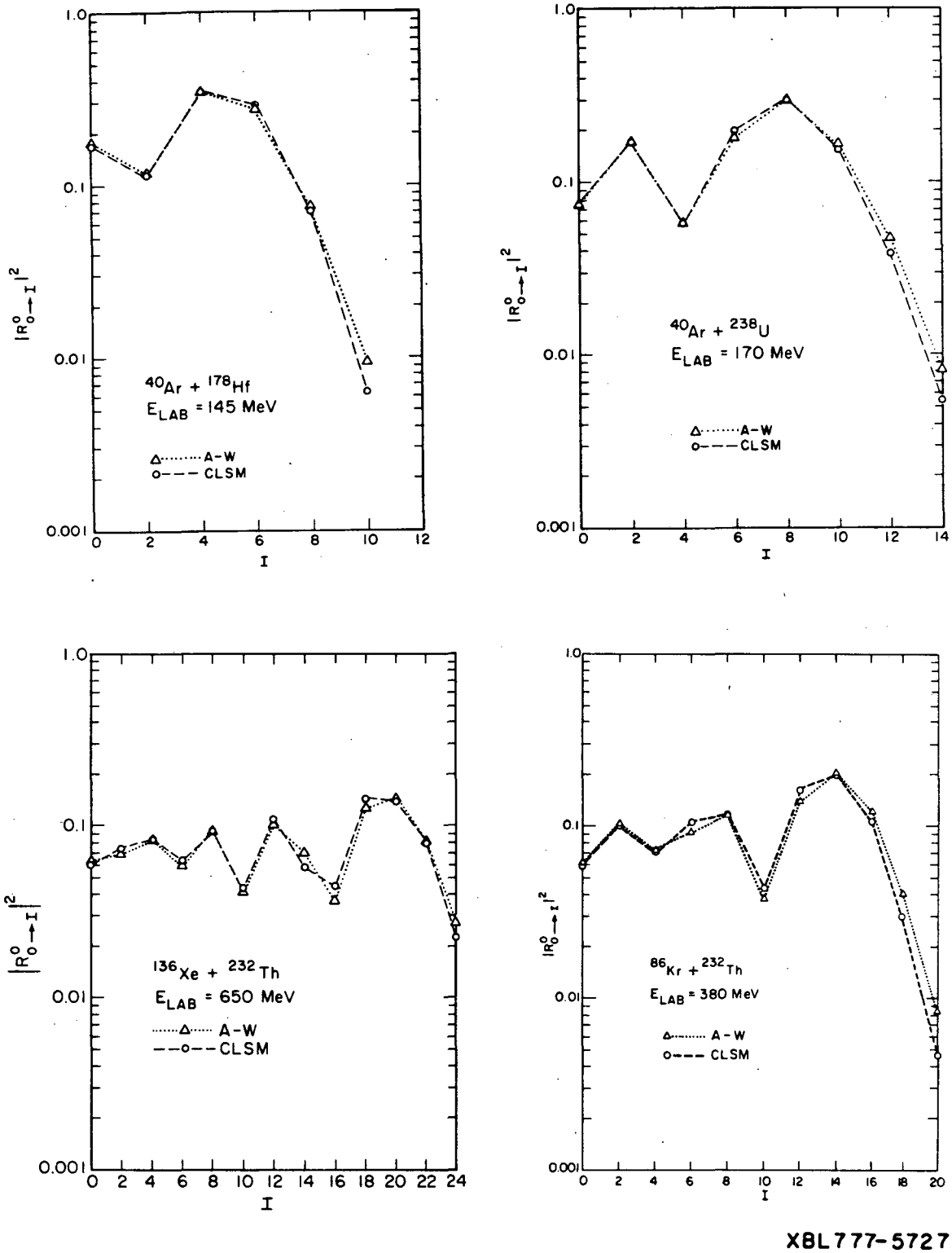
$^{40}Ar + ^{178}Hf$
E_{LAB} = 145 MeV
A-W
CLSM
$^{40}Ar + ^{238}U$
E_{LAB} = 170 MeV
A-W
CLSM
$^{136}Xe + ^{232}Th$
E_{LAB} = 650 MeV
A-W
CLSM
$^{86}Kr + ^{232}Th$
E_{LAB} = 380 MeV
A-W
CLSM
$|R^0_{0\to I}|^2$
I
XBL777-5727

Fig. 11

TECHNICAL INFORMATION DIVISION
LAWRENCE BERKELEY LABORATORY
UNIVERSITY OF CALIFORNIA
BERKELEY, CALIFORNIA 94720